Supplementary Information for

Pressure-dependent Helix Inversion of Poly(quinoxaline2,3-diyl)s Containing Chiral Side Chains in Non-aqueous Solvents

Yuuya Nagata,*[a] Ryohei Takeda,[a] and Michinori Suginome*[ab]

[a] Department of Synthetic Chemistry and Biological Chemistry,

Graduate School of Engineering, Kyoto University, Kyoto 606-8501, Japan

[b] CREST, Japan Science and Technology Agency (JST),

Katsura, Nishikyo-ku, Kyoto 615-8510, Japan

E-mail: nagata@sbchem.kyoto-u.ac.jp, suginome@sbchem.kyoto-u.ac.jp

1. General

All reactions were carried out under an atmosphere of nitrogen with magnetic stirring. ^{1}H NMR spectra were recorded on a Varian 400-MR spectrometer at ambient temperature. ^{1}H NMR data are reported as follows: chemical shift in ppm downfield from tetramethylsilane (δ scale), multiplicity (s = singlet, d = doublet, t = triplet, m = multiplet and br = broad), coupling constant (Hz), and integration. The GPC analysis was carried out with TSKgel G4000H_{HR} or TSKgel GMH_{XL} ($CHCl_3$, polystyrene standards). Preparative GPC was performed on JAI LC-908 equipped with JAIGEL-1H and - 2H columns in a series ($CHCl_3$). CD spectra were recorded on a JASCO J-750 spectrometer equipped with a high-pressure cell at room temperature. UV spectra were calculated from HT voltage measured with spectrometer.
o-TolNiCl(PMe_3)$_2$,[1] **1m**,[2] **2m**,[3] **3m**,[3] and **4m**,[4] were prepared according to the reported procedures. Tetrahydrofurane (THF) were dried and deoxygenized using an alumina/catalyst column system (Glass Contour Co.). Other chemical reagents were purchased from the commercial sources and were used without further purification.

2. Experimental Procedures and Spectral Data for Synthesized Compounds

Synthesis of 1 : A THF solution of *o*-TolNiCl(PMe$_3$)$_2$ (50.0 mM, 45.7 µL, 2.28 µmol) was diluted with THF (3 mL). **1m** (30.0 mg, 91.3 µmol) were dissolved in THF (3 mL). A THF solution of *o*-TolNiCl(PMe$_3$)$_2$ (6.43 mM, 391.9 µL, 2.52 µmol) was added to the monomer solution. After 19.5 h, A THF solution of LiBH$_4$ (2.00 M, 182.7 µL, 91.3 µmol) was added to the reaction mixture and stirred for 1 h. Saturated NH$_4$Cl aq (10 mL) was added to the solution and extracted with and CH$_2$Cl$_2$ (10 ml). The organic extract was washed with water (10 mL) and brine (10 mL), dried over Na$_2$SO$_4$, and the solvent was evaporated. The residue was subjected to preparative GPC to give **1** as a beige solid (29.9 mg, >99%). ^{1}H NMR (CDCl$_3$) 4.62 (2H, br s), 4.53 (2H, br s), 3.40 (2H, br s), 2.31 (6H, br s), 1.21 (6H, br, d J = 4.8 Hz), 0.87(6H, br, t J = 6.6 Hz); GPC (CHCl$_3$, g/mol): $M_n = 7.35 \times 10^3$, $M_w/M_n = 1.13$.

Scheme S1. Synthesis of **1**.

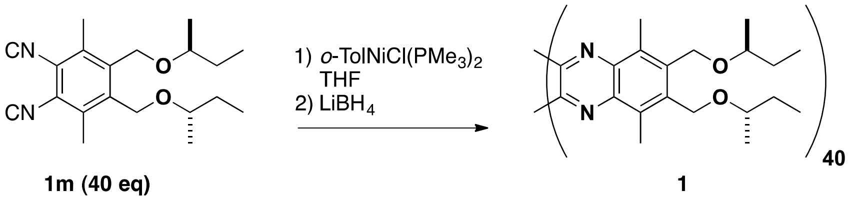

Synthesis of 2 : A THF solution of *o*-TolNiCl(PMe$_3$)$_2$ (50.6 mM, 34.6 µL, 1.75 µmol) was diluted with THF (3 mL). **2m** (25.0 mg, 70.1 µmol) was dissolved in THF (3 mL). A THF solution of *o*-TolNiCl(PMe$_3$)$_2$ (9.34 mM, 223.6 µL, 2.09 µmol) was added to the monomer solution. After stirring for 17 h, a NaBH$_4$ (5.30 mg, 140 µmol) was added to the reaction mixture at room temperature. After stirring for 1 h at room temperature, saturated NH$_4$Claq (1 mL) was added. Extraction with CH$_2$Cl$_2$ (10mL) followed by preparative GPC gave **2** as a beige solid (24.9 mg, >99%). ^{1}H NMR (CDCl$_3$) δ 4.65 (2H, br s), 4.48 (2H, br s), 3.46 (2H, br s), 2.57–2.01 (14H, m), 1.79–1.03 (14H, m), 0.99–0.73 (6H, m); GPC ($CHCl_3$, g/mol): $M_n = 6.59 \times 10^3$, $M_w/M_n = 1.14$.

Scheme S2. Synthesis of **2**.

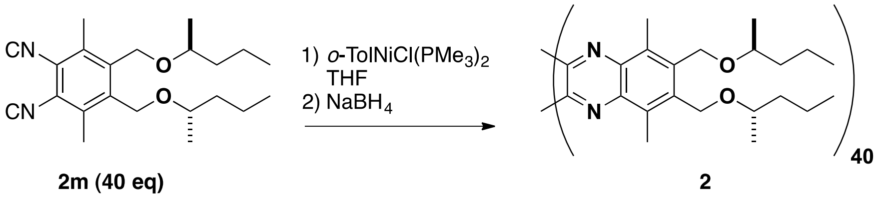

Synthesis of 3 : A THF solution of *o*-TolNiCl(PMe_3)$_2$ (50.0 mM, 52.3 µL, 2.61 µmol) was diluted with THF (3 mL). A THF solution of **3m** (46.0 mg, 104 µmol) was diluted with THF (3 mL). The monomer solution was added to the solution of *o*-TolNiCl(PMe_3)$_2$. After stirring for 12 h, $NaBH_4$ (7.87 mg, 208 µmol) was added to the reaction mixture at room temperature. After stirring for 1 h at room temperature, saturated NH_4Cl aq (10 mL) was added and extracted with CH_2Cl_2 (10 mL). The organic extract was washed with water (10 mL) and brine (10 mL) and dried over Na_2SO_4 followed by preparative GPC gave **3** as a beige solid (43.2 mg, 94%). ^{1}H NMR ($CDCl_3$) δ 4.62 (2H, br s), 4.50 (2H, br s), 3.47 (2H, br s), 2.54–1.97 (6H, m), 1.75–0.99 (28H, m), 0.84 (6H, br s); GPC ($CHCl_3$, g/mol): $M_n = 8.06 \times 10^3$, $M_w/M_n = 1.13$.

Scheme S3. Synthesis of **3**.

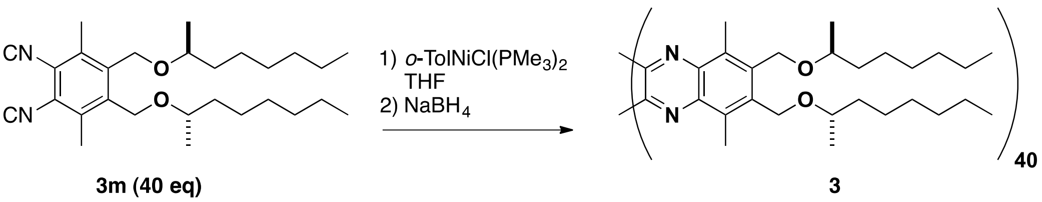

Synthesis of 4 : A THF solution of *o*-TolNiCl(PMe_3)$_2$ (50.0 mM, 15.2 µL, 0.76 µmol) was diluted with THF (3 mL). A THF solution of **4m** (11.8 mg, 30.4 µmol) was diluted with THF (3 mL). The monomer solution was added to the solution of *o*-TolNiCl(PMe_3)$_2$. After stirring for 11 h, $NaBH_4$ (2.31 mg, 61 µmol) was added to the reaction mixture at room temperature. After stirring for 1 h at room temperature, saturated NH_4Cl aq (10 mL) was added and extracted with CH_2Cl_2 (10 mL). The organic extract was washed with water (10 mL) and brine (10 mL) and dried over Na_2SO_4 followed by preparative GPC gave **4** as a beige solid (10.7 mg, 91%). ^1H NMR ($CDCl_3$) δ 4.98 (2H, br s), 4.63 (2H, br s), 4.13 (2H, br s), 3.74–3.53 (6H, m), 2.60–2.07 (6H, m), 1.36 (6H, br s); GPC ($CHCl_3$, g/mol): $M_n = 9.39 \times 10^3$, $M_w/M_n = 1.17$.

Scheme S4. Synthesis of **4**.

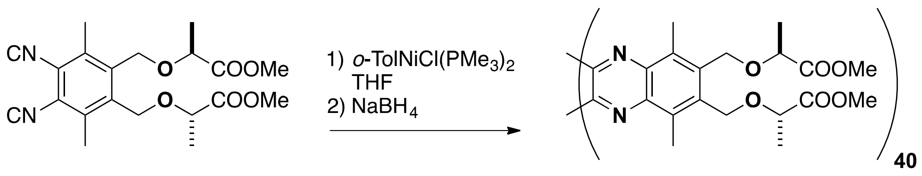

4m (40 eq)

4

Synthesis of 1(60) : A THF solution of *o*-TolNiCl(PMe_3)$_2$ (50.0 mM, 50.8 µL, 2.54 µmol) was diluted with THF (3 mL). A THF solution of **1m** (50.0 mg, 152 µmol) was diluted with THF (3 mL). The monomer solution was added to the solution of *o*-TolNiCl(PMe_3)$_2$. After stirring for 12 h, $LiBH_4$ (2.00 M, 304 µL, 152 µmol) was added to the reaction mixture at room temperature. After stirring for 1 h at room temperature, saturated NH_4Cl aq (10 mL) was added and extracted with CH_2Cl_2 (10 mL). The organic extract was washed with water (10 mL) and brine (10 mL) and dried over Na_2SO_4 followed by preparative GPC gave **1(60)** as a beige solid (49.4 mg, 99%). ^1H NMR ($CDCl_3$) 4.64 (2H, br s), 4.51 (2H, br s), 3.39 (2H, br s), 2.32 (6H, br s), 1.68–1.31 (4H, m), 1.21 (6H, br, d $J = 4.56$ Hz), 0.87(6H, br, t $J = 6.72$ Hz); GPC ($CHCl_3$, g/mol): $M_n = 12.2 \times 10^3$, $M_w/M_n = 1.11$. **1(60)** was soluble in 1,2-DCE under 0.1 MPa and insoluble in 1,2-DCE under 200 MPa.

Scheme S5. Synthesis of **1(60)**.

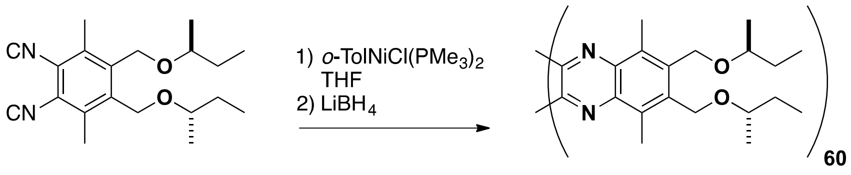

1m (60 eq)

1(60)

Synthesis of 1(100) : A THF solution of *o*-TolNiCl(PMe3)$_2$ (50.0 mM, 62.4 µL, 3.12 µmol) was diluted with THF (3 mL). A THF solution of **1m** (102 mg, 312 µmol) was diluted with THF (3 mL). The monomer solution was added to the solution of *o*-TolNiCl(PMe_3)$_2$. After stirring for 18h, $LiBH_4$ (2.00 M, 623 µL, 312 µmol) was added to the reaction mixture at room temperature. After stirring for 1 h at room temperature, saturated NH_4Cl aq (10 mL) was added and extracted with CH_2Cl_2 (10 mL). The organic extract was washed with water (10 mL) and brine (10 mL) and dried over Na_2SO_4 followed by preparative GPC gave **1(100)** as a beige solid (98.5 mg, 96%). ^{1}H NMR ($CDCl_3$) 4.64 (2H, br s), 4.55 (2H, br s), 3.40 (2H, br s), 2.32 (6H, br s), 1.72–1.33 (4H, m), 1.21 (6H, br s), 0.88(6H, br s); GPC ($CHCl_3$, g/mol): $M_n = 27.8 \times 10^3$, M_w/M_n = 1.08. **1(100)** was insoluble in 1,2-DCE.

Scheme S6. Synthesis of **1(100)**.

1m (100 eq)

1(100)

Synthesis of 1(200) : A THF solution of *o*-TolNiCl(PMe_3)$_2$ (50.0 mM, 30.4 µL, 1.52 µmol) was diluted with THF (3 mL). A THF solution of **1m** (99.8 mg, 303 µmol) was diluted with THF (3 mL). The monomer solution was added to the solution of *o*-TolNiCl(PMe_3)$_2$. After stirring for 19 h, $LiBH_4$ (2.00 M, 608 µL, 304 µmol) was added to the reaction mixture at room temperature. After stirring for 1 h at room temperature, saturated NH_4Cl aq (10 mL) was added and extracted with CH_2Cl_2 (10 mL). The organic extract was washed with water (10 mL) and brine (10 mL) and dried over Na_2SO_4 followed by preparative GPC gave **1(200)** as a beige solid (94.3 mg, 94%). ^{1}H NMR ($CDCl_3$) 4.65 (4H, br s), 3.41 (2H, br s), 2.32 (6H, br s), 1.78–1.34 (4H, m), 1.34–1.05 (6H, m), 0.88(6H, br s); GPC ($CHCl_3$, g/mol): $M_n = 55.1 \times 10^3$, M_w/M_n = 1.25. **1(200)** was insoluble in 1,2-DCE.

Scheme S7. Synthesis of **1(200)**.

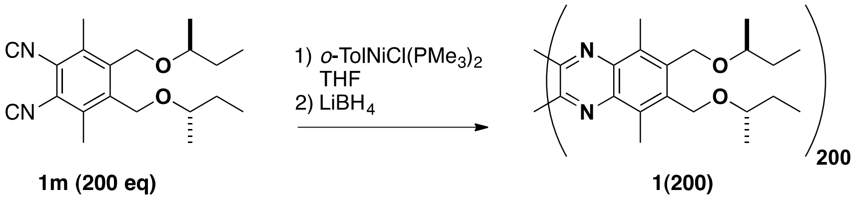

3. High-pressure CD and UV-vis measurement

General procedure: A polymer was dissolved in solvent (ca. 0.1 g/L) to enclose a quartz inner cell (volume = 300 μL, light path length = 2 mm) with a diaphragm tube. The inner cell was placed in a high-pressure vessel with quartz windows (PCI-500, Syn Corporation, Kyoto, Japan) to be pressurized by a high-pressure hand pump (HP-500, Syn Corporation, Kyoto, Japan) using water as pressure medium. The high-pressure vessel was set in JASCO J-750 spectrometer to measure CD and UV-vis spectra. Absorbance (A) was calculated from voltage value (HT) of a photomultiplier tube in the spectrometer according to the following equation, whose validity was also confirmed by comparing the obtained spectra with UV-vis spectra measured by JASCO V-770 UV-Visible/NIR spectrophotometer.

$$A = \{a \times (HT)^4\} + \{b \times (HT)^3\} + \{c \times (HT)^2\} + \{d \times HT\} + e, \qquad (1)$$

Here, $a = -5.933 \times 10^{-12}$, $b = 2.265 \times 10^{-8}$, $c = -3.179 \times 10^{-5}$, $d = 2.424 \times 10^{-2}$, $e = -3.720$.

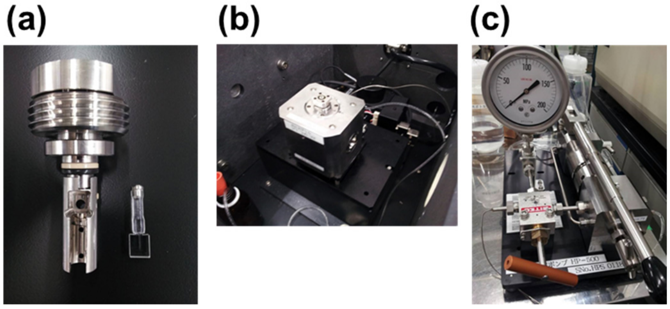

Figure S1. Photographs of (a) a quartz inner cell and a cell holder (b) a high-pressure vessel with quartz windows (c) a high-pressure hand pump with a pressure gauge.

Determination of rate constants: We supposed that the helix inversion induced by pressure is a first order reaction to determine the rate constants, i.e., we adopted following equation for curve fittings. The g_{abs} plot against time was subjected to a nonlinear, least-squares fitting of the parameters a, c, t_0, and k (the rate constant) using the following equation.

$$g_{\mathrm{abs}} = a \times \exp\{-k \times (t - t_0)\} + c, \quad (2)$$

These parameters were successfully converged (Figure S2) and the final values are summarized in Table 1. We concluded that rate constants for the helix inversion reaction were determined as $2.40 \times 10^{-2}\ \mathrm{s}^{-1}$ (P to M at 200 MPa) and $5.41 \times 10^{-3}\ \mathrm{s}^{-1}$ (M to P at 0.1 MPa) after averaging the obtained values.

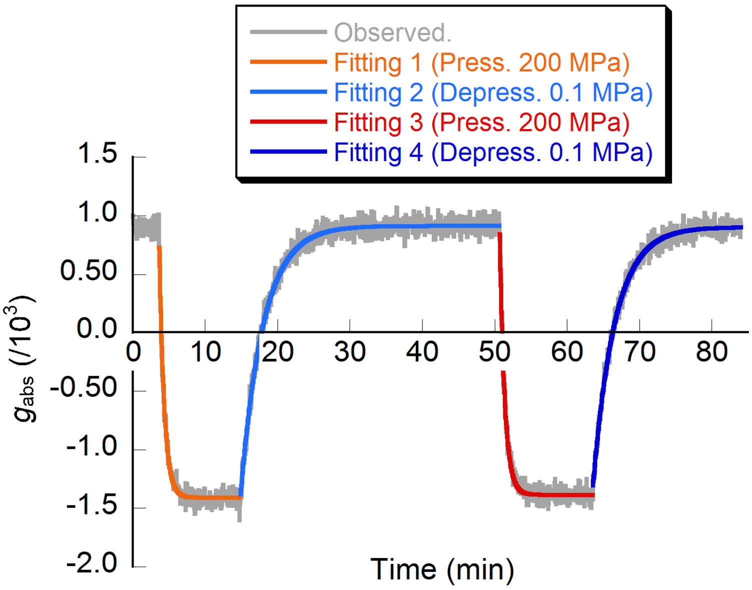

Figure S2. Time-resolved CD intensity change of **1** in 1,2-DCE at 368.0 nm exposed to pressurization (200 MPa) and depressurization (0.1 MPa) cycles. Fitting curves are also presented. Data points observed within a few seconds after pressurization were omitted from the curve fittings to exclude errors arising from the time of the pressurization and the temporal temperature change.

Table 1. Converged values of a, c, t_0, and k in pressurization (200 MPa) and depressurization (0.1 MPa) cycles.

Fitting	a (/10^3)	c (/10^3)	t_0 (min)	k (s^{-1})
1 (Press.)	1.03	–1.41	4.15	2.43×10^{-2}
2 (Depress.)	–1.97	0.91	15.38	5.33×10^{-3}
3 (Press.)	1.00	–1.39	51.26	2.37×10^{-2}
4 (Depress.)	–2.04	0.90	63.85	5.49×10^{-3}

Determination of the difference of the partial molar volume of the dissolved polymer and the compressibility factor: According to Hawley,[5] the Gibbs energy difference (ΔG) in an isothermal process before and after pressurization can be expressed as

$$\Delta G = \Delta V \times (P - P_0) - \Delta\beta/2 \times (P - P_0)^2, \qquad (3)$$

where ΔV and Δβ represent the difference of the partial molar volume of the dissolved polymer and the compressibility factor, respectively. According to Green's theory,[6] ΔG of the helix inversion may also be expressed as

$$\Delta G = -2RT_0 \times \{\mathrm{atanh}(g_{\mathrm{abs}} / g_{\mathrm{max}}) - \mathrm{atanh}(g_{\mathrm{abs,0}} / g_{\mathrm{max}})\}, \qquad (4)$$

wherein $g_{\mathrm{abs,0}}$ and g_{abs} refer to the dissymmetry factor before and after pressurization, respectively, g_{max} to the dissymmetry factor for the purely single-handed polymer (P-helix, 100%, 2.31×10^{-3} was used here), T_0 to the operating temperature (298.15 K), and R to the gas constant (8.314 J K^{-1} mol^{-1}). Therefore, g_{abs} can be expressed using P as

$$g_{\mathrm{abs}} = \tanh[\{\Delta V \times (P - P_0) - \Delta\beta/2 \times (P - P_0)^2\}/(-2RT_0) + \mathrm{atanh}(g_{\mathrm{abs,0}} / g_{\mathrm{max}})], \qquad (4)$$

After nonlinear least-squares fitting, convergence of these parameters at $\Delta V = -36.8$ cm^3 mol^{-1} and $\Delta\beta = -0.103$ cm^3 mol^{-1} MPa^{-1} were observed.

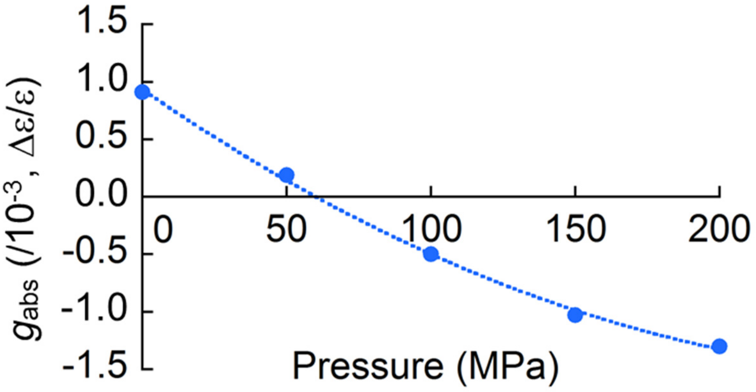

Figure S3. Correlation between pressure and g_{abs} of **1** in 1,2-DCE at 368.0 nm. A fitted curve was also presented.

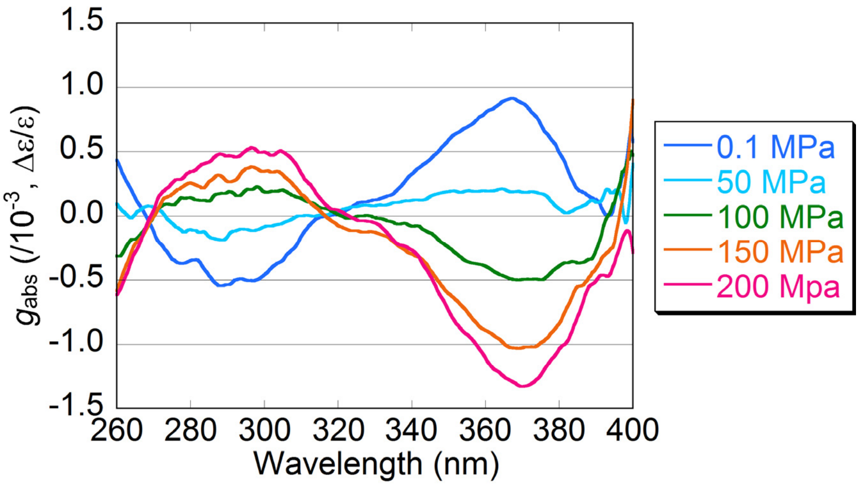

Figure S4. CD spectra of **1** in 1,2-DCE at various pressures (14.5×10^{-2} g/L, light path length = 2 mm).

4. References

1. Carmona, E.; Paneque, M.; Poveda, M. L. *Polyhedron* **1989**, *8*, 285.
2. Yamada, T; Nagata, Y.; Suginome, M. *Chem. Commun.* **2010**, *46*, 4914
3. Nagata, Y.; Yamada, T.; Adachi, T.; Akai, Y.; Yamamoto, T.; Suginome, M. *J. Am. Chem. Soc.*, **2013**, *135*, 10104.
4. Nagata, Y.; Kuroda, T.; Takagi, K.; Suginome, M. *Chem. Sci.* **2014**, *5*, 4953.
5. Hawley, S. A. *Biochemistry*, **1971**, *10*, 2436.
6. Lifson, S.; Andreola, C.; Peterson, N. C.; Green, M. M. *J. Am. Chem. Soc.*, **1989**, *111*, 8850.

5. NMR Spectra of New Compounds

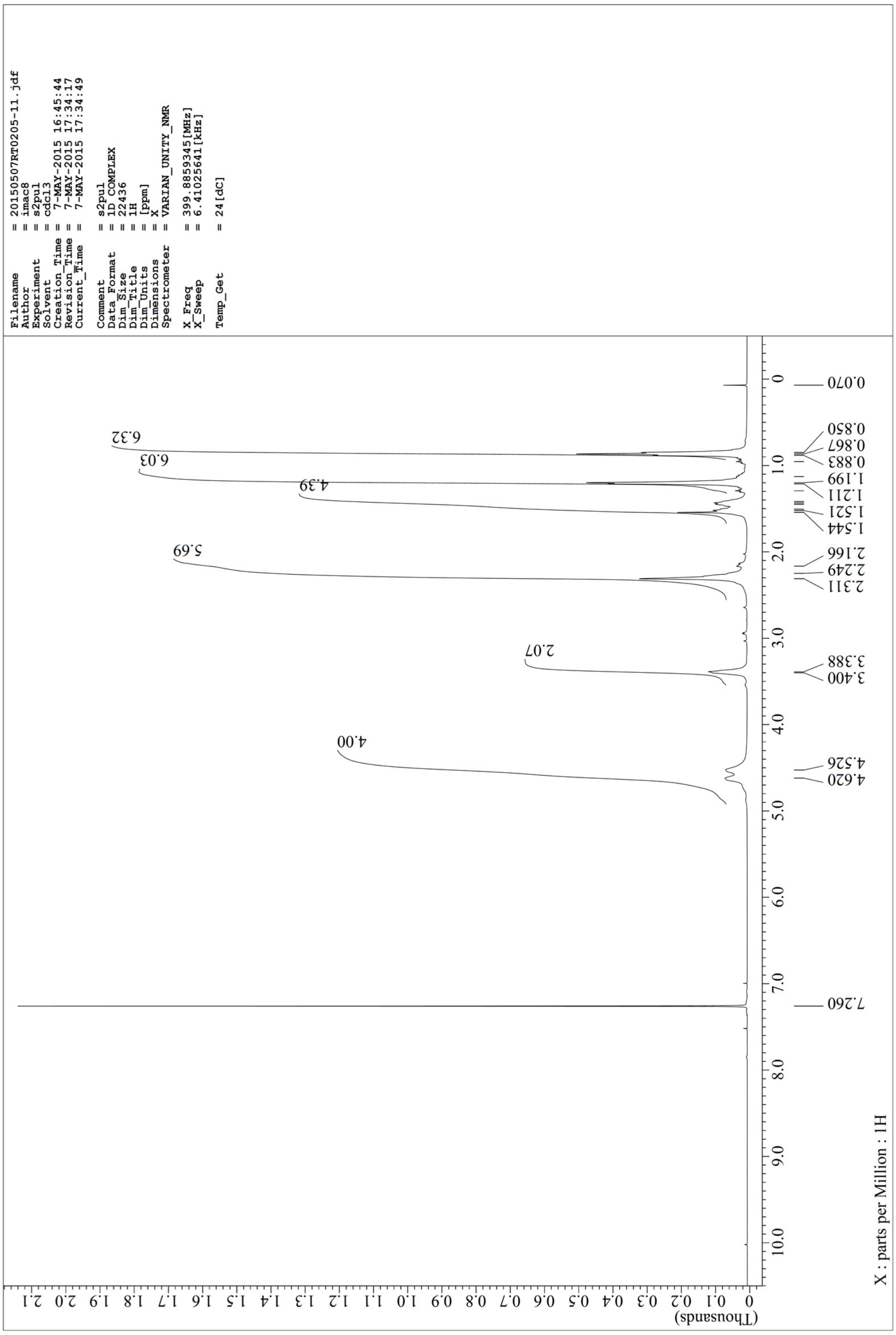

Figure S5. ^{1}H NMR spectrum of **1** in $CDCl_3$.

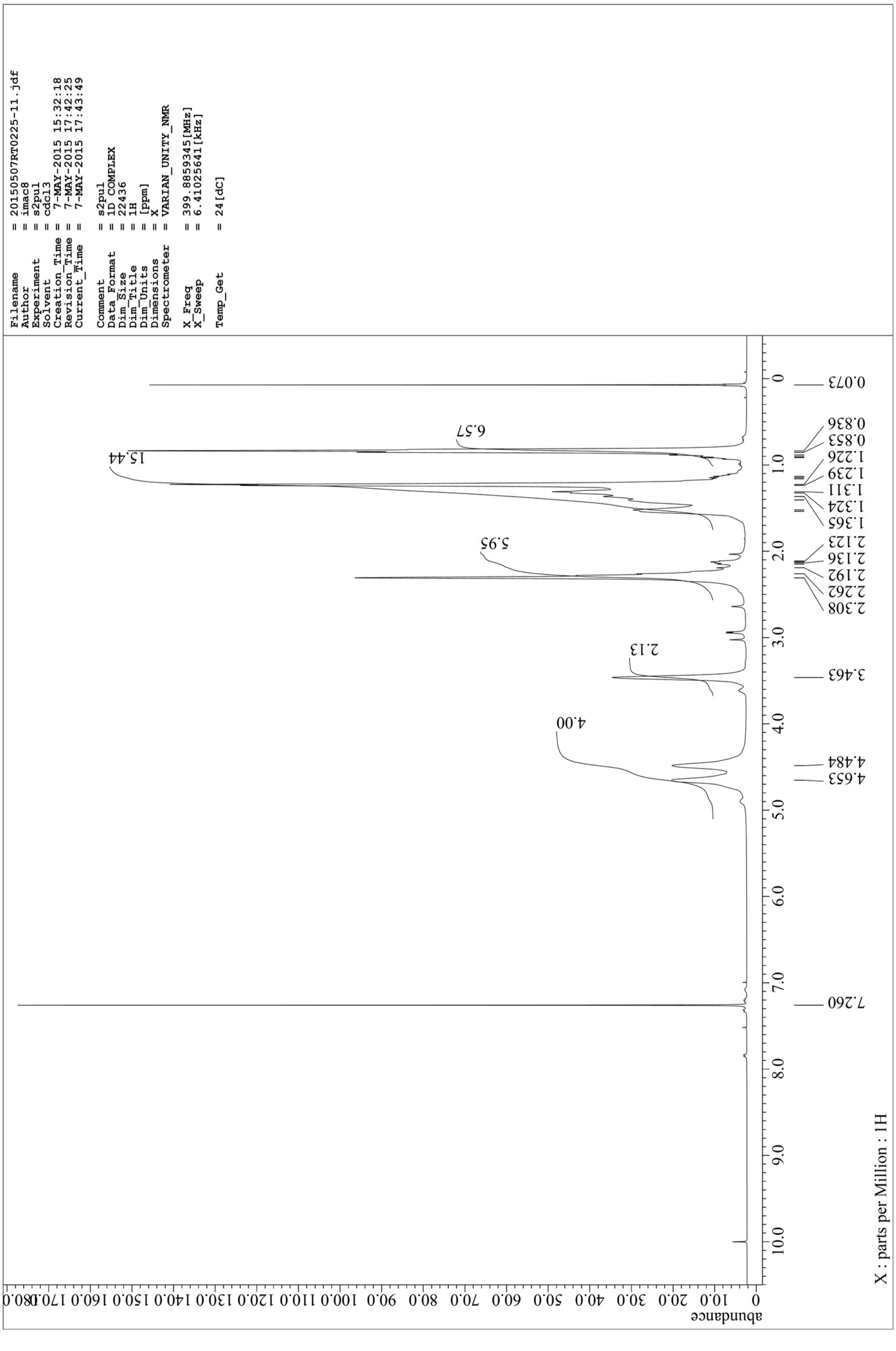

Figure S6. ^{1}H NMR spectrum of **2** in $CDCl_3$.

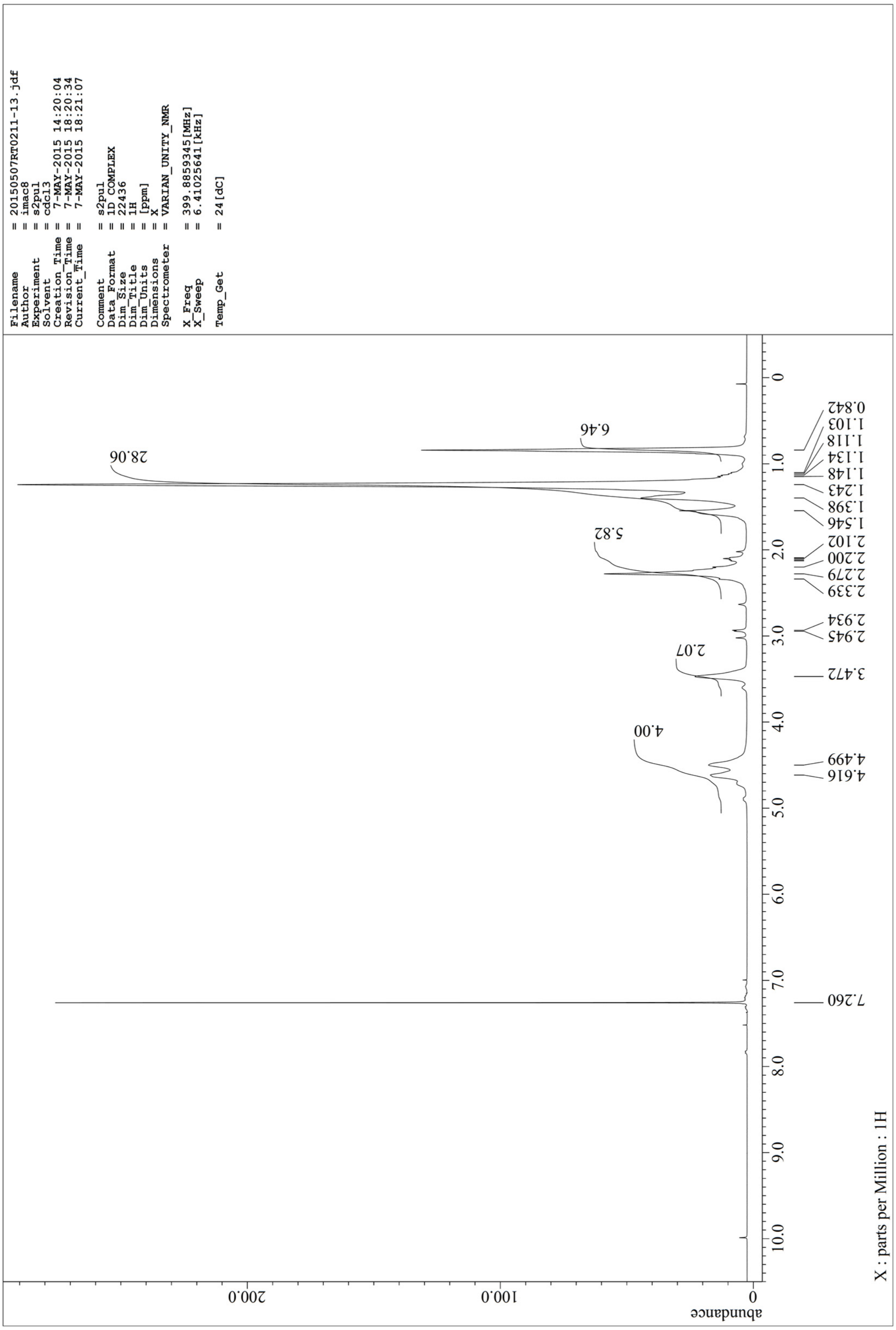

Figure S7. ^{1}H NMR spectrum of **3** in $CDCl_3$.

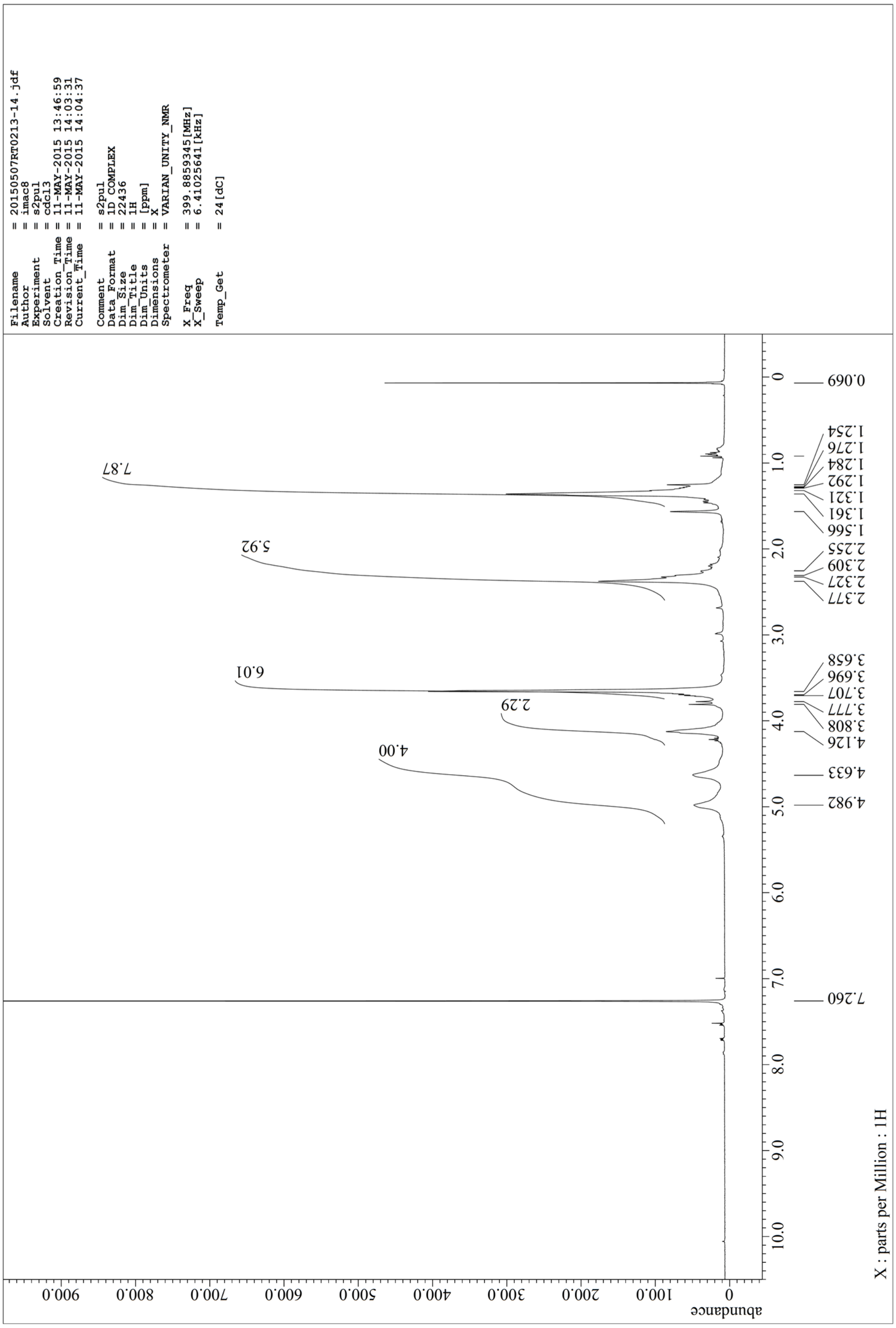

```
Filename        = 20150507RT0213-14.jdf
Author          = imac8
Experiment      = s2pul
Solvent         = cdcl3
Creation_Time   = 11-MAY-2015 13:46:59
Revision_Time   = 11-MAY-2015 14:03:31
Current_Time    = 11-MAY-2015 14:04:37

Comment         = s2pul
Data_Format     = 1D COMPLEX
Dim_Size        = 22436
Dim_Title       = 1H
Dim_Units       = [ppm]
Dimensions      = X
Spectrometer    = VARIAN_UNITY_NMR

X_Freq          = 399.8859345[MHz]
X_Sweep         = 6.41025641[kHz]

Temp_Get        = 24[dC]
```

Figure S8. ^{1}H NMR spectrum of **4** in $CDCl_3$.

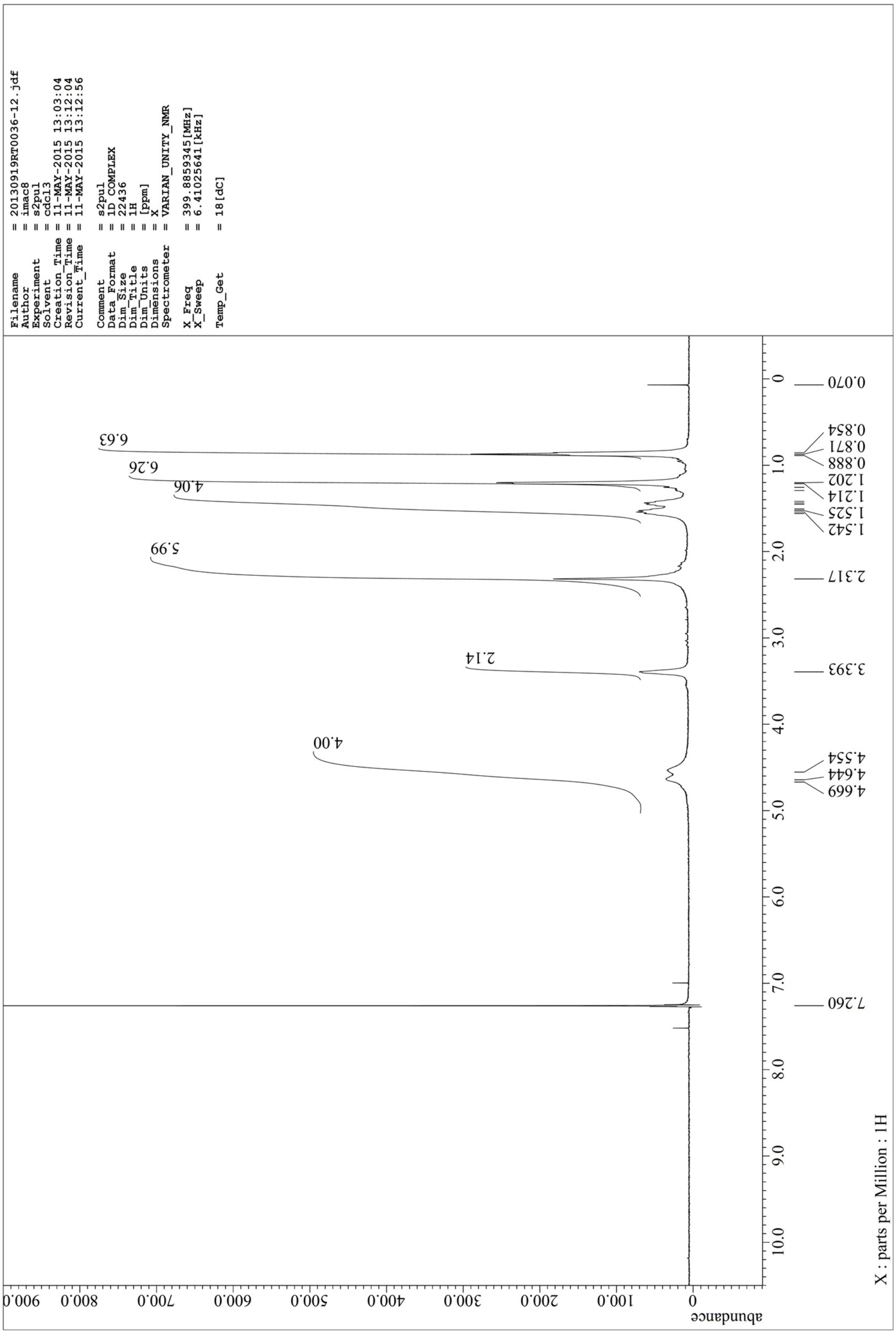

Figure S9. ^{1}H NMR spectrum of **1_60** in CDCl$_3$.

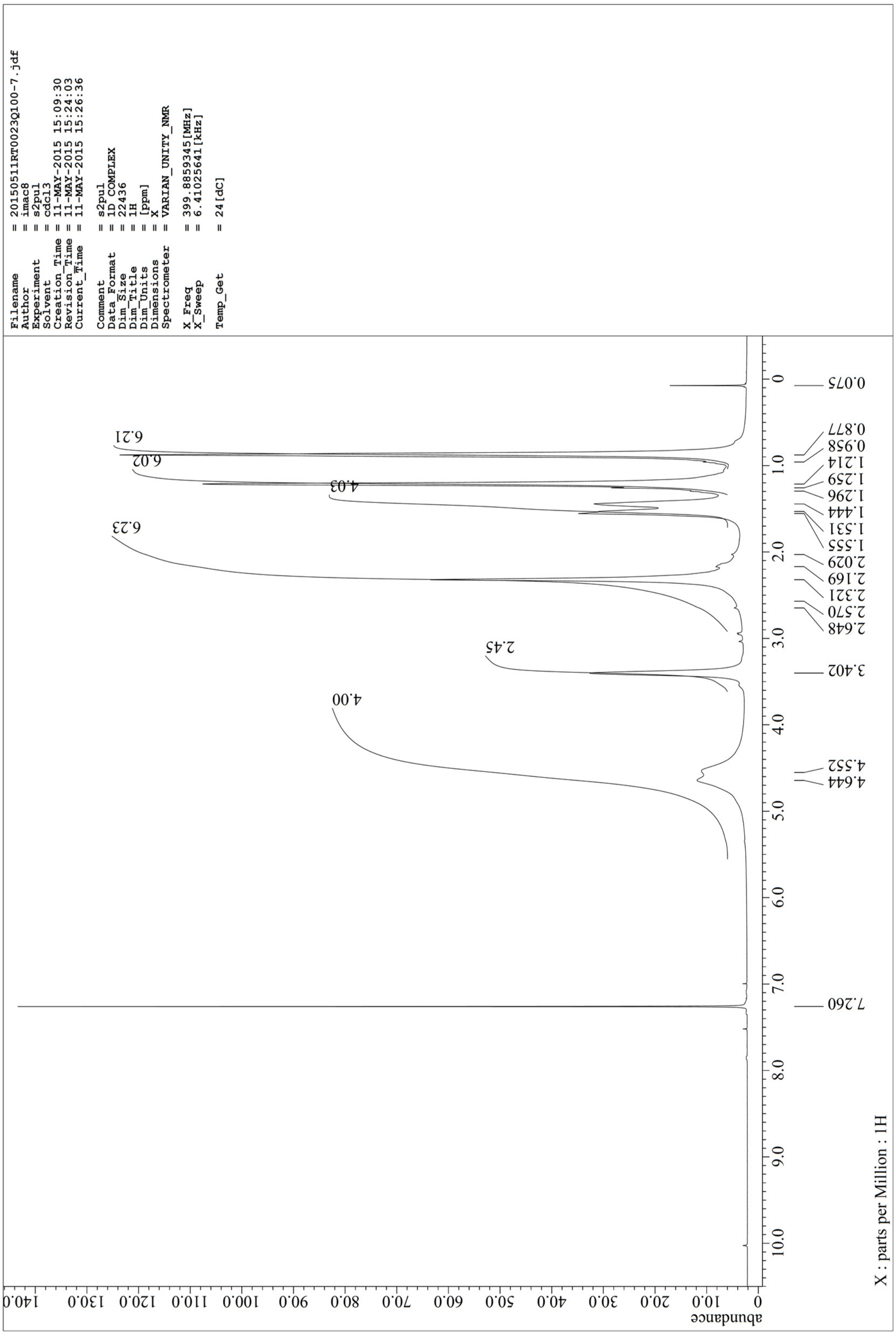

Figure S10. ^{1}H NMR spectrum of **1_100** in $CDCl_3$.

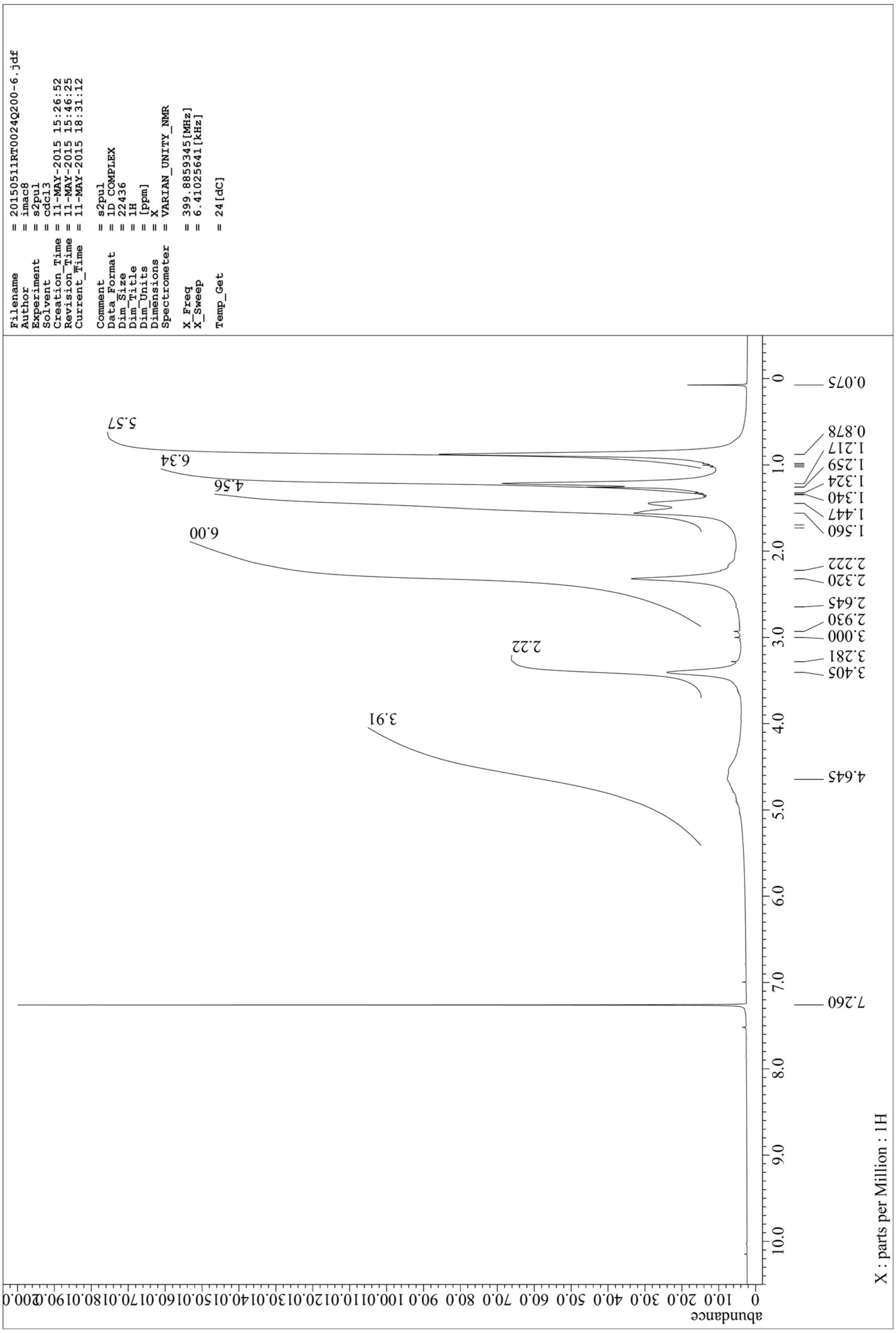

Figure S11. ^{1}H NMR spectrum of **1_200** in $CDCl_3$.

6. UV-vis and CD spectra of New Compounds

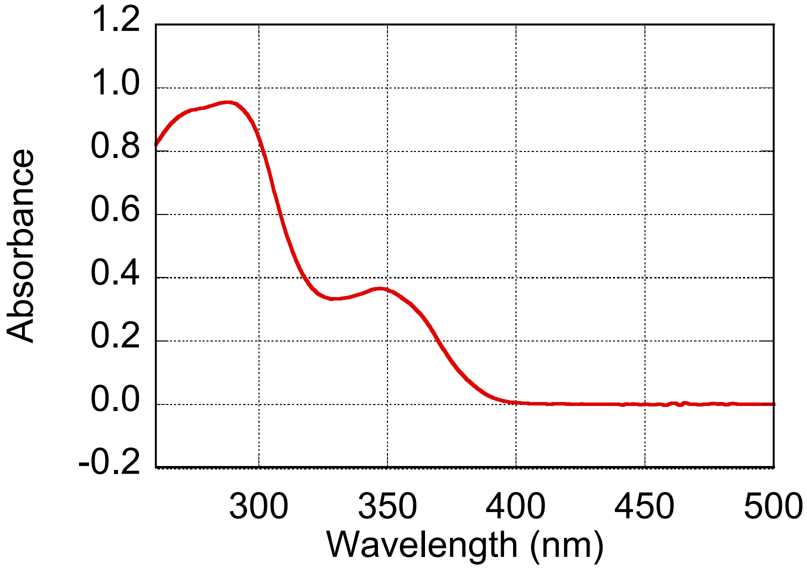

Figure S12. UV-vis absorption of **1(60)** in 1,2-DCE under 0.1 MPa (8.60×10^{-2} g/L, light path length = 2 mm).

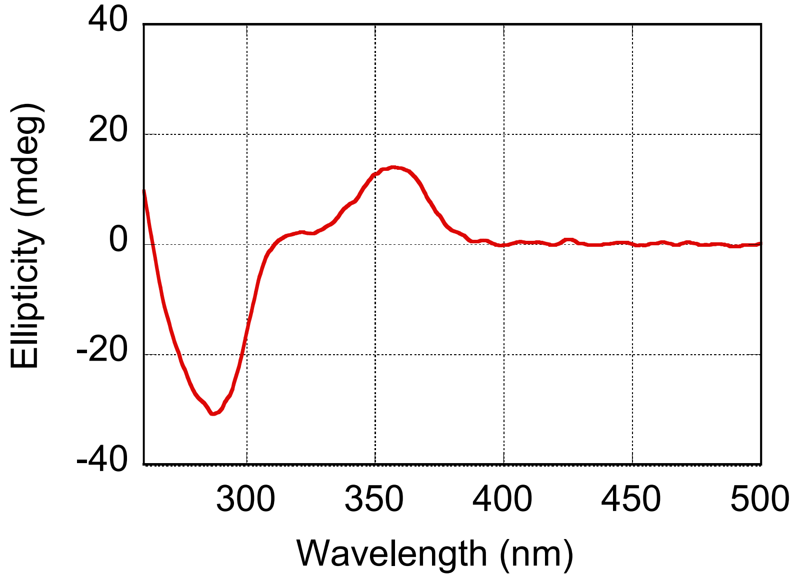

Figure S13. CD spectrum of **1(60)** in 1,2-DCE under 0.1 MPa (8.60×10^{-2} g/L, light path length = 2 mm).

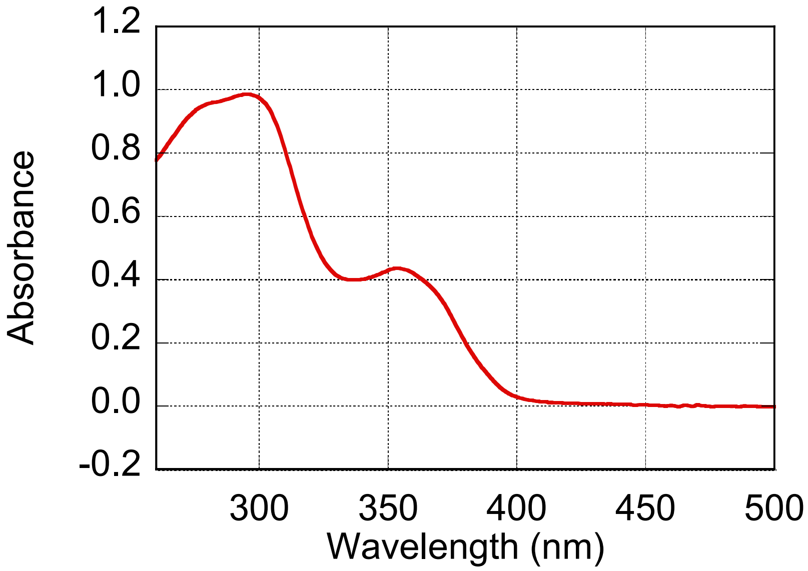

Figure S14. UV-vis absorption of **1(60)** in 1,2-DCE under 200 MPa (8.60×10^{-2} g/L, light path length = 2 mm).

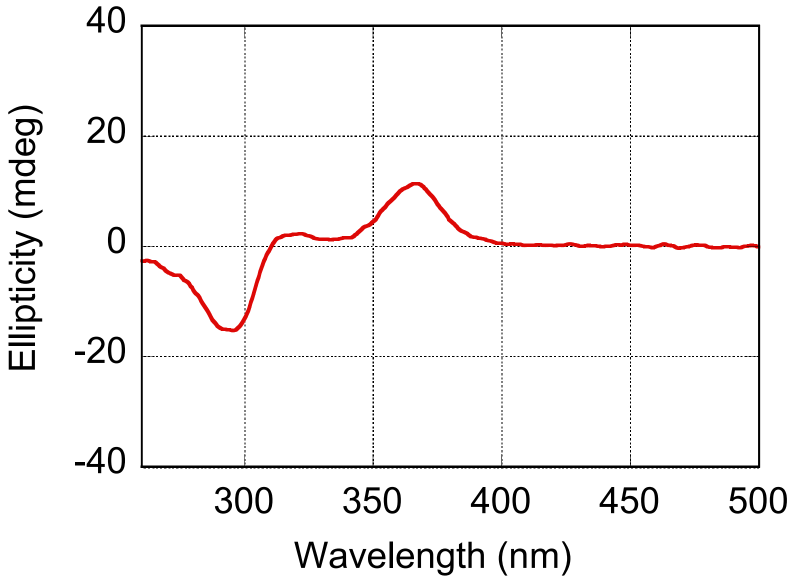

Figure S15. CD spectrum of **1(60)** in 1,2-DCE under 200 MPa (8.60×10^{-2} g/L, light path length = 2 mm).

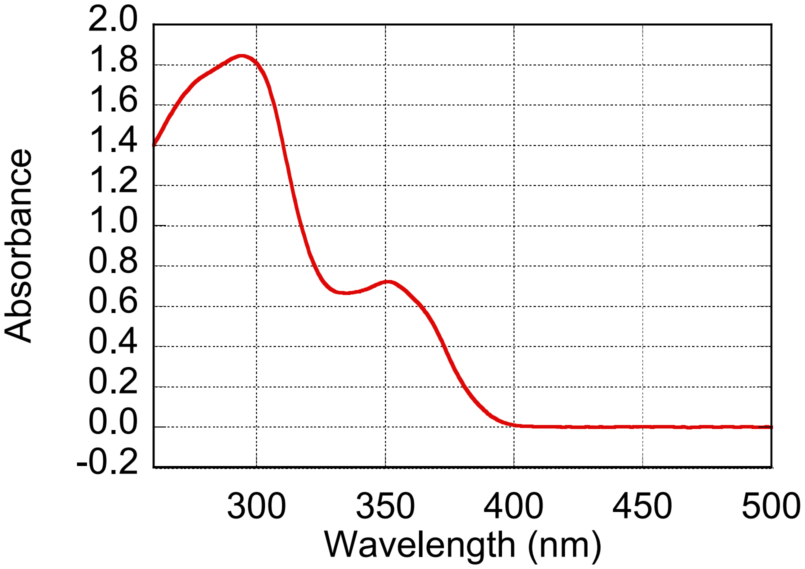

Figure S16 UV-vis absorption of **1** in $CHCl_3$ under 0.1 MPa
(12.2 × 10^{-2} g/L, light path length = 2 mm).

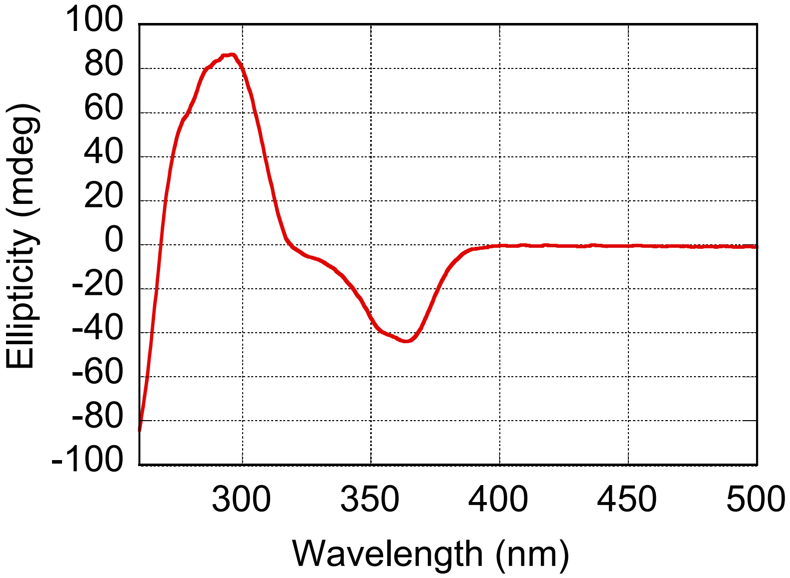

Figure S17. CD spectrum of **1** in $CHCl_3$ under 0.1 MPa
(12.2 × 10^{-2} g/L, light path length = 2 mm).

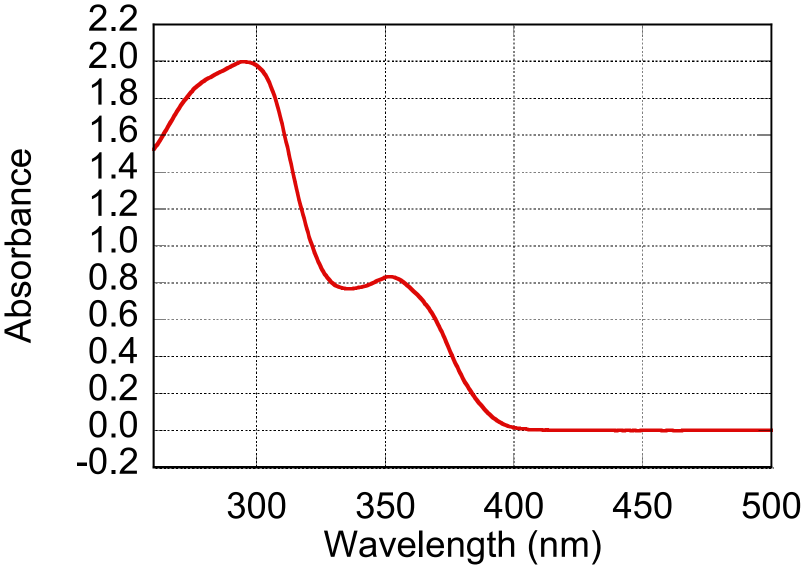

Figure S18. UV-vis absorption of **1** in $CHCl_3$ under 200 MPa (12.2×10^{-2} g/L, light path length = 2 mm).

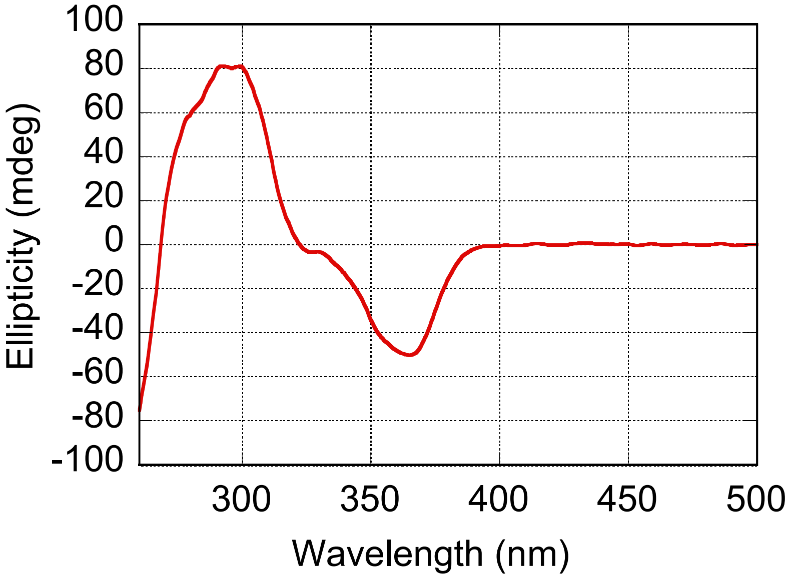

Figure S19. CD spectrum of **1** in $CHCl_3$ under 200 MPa (12.2×10^{-2} g/L, light path length = 2 mm).

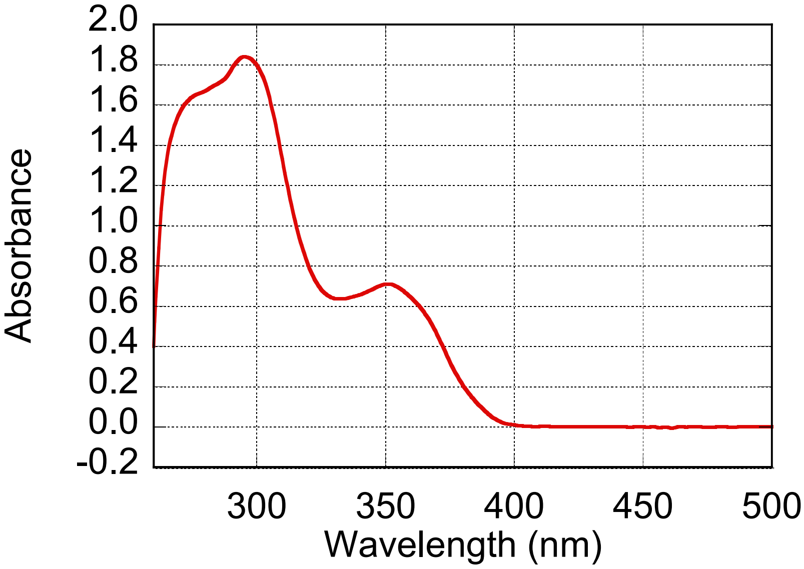

Figure S20. UV-vis absorption of **1** in 1,1,2-TCE under 0.1 MPa (16.3×10^{-2} g/L, light path length = 2 mm).

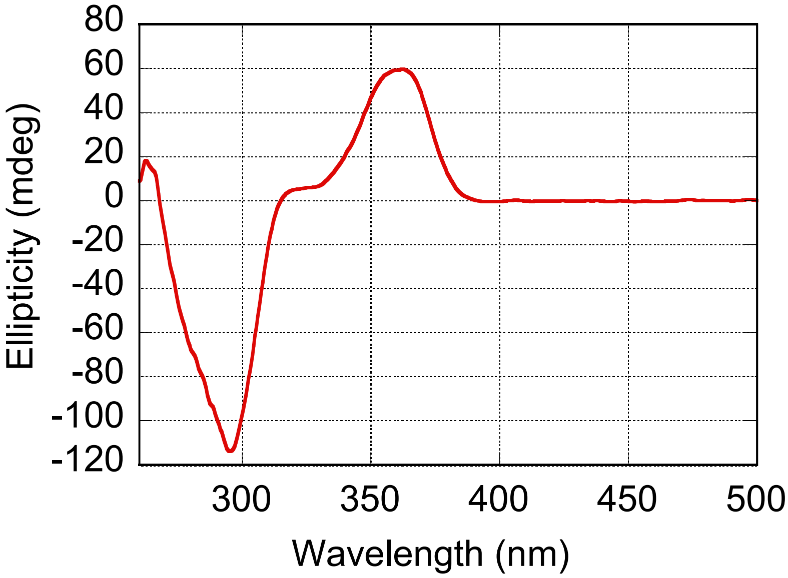

Figure S21. CD spectrum of **1** in 1,1,2-TCE under 0.1 MPa (16.3×10^{-2} g/L, light path length = 2 mm).

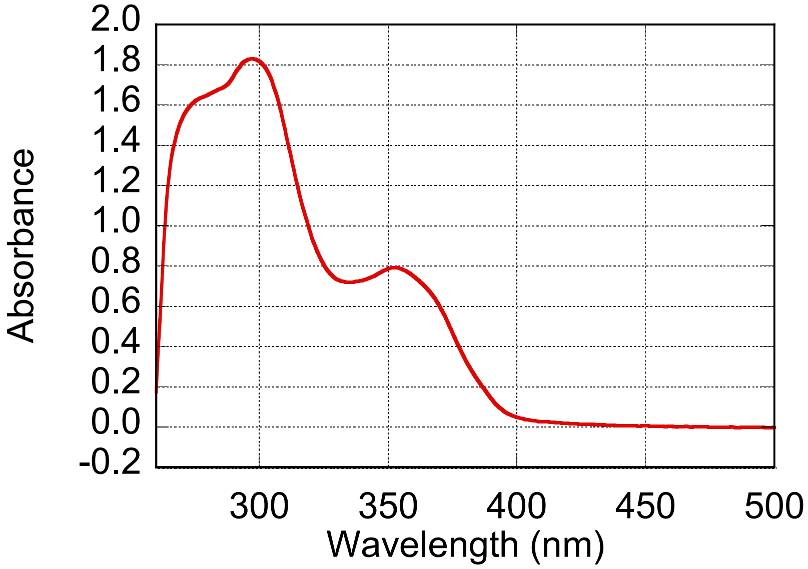

Figure S22. UV-vis absorption of **1** in 1,1,2-TCE under 200 MPa (16.3×10^{-2} g/L, light path length = 2 mm).

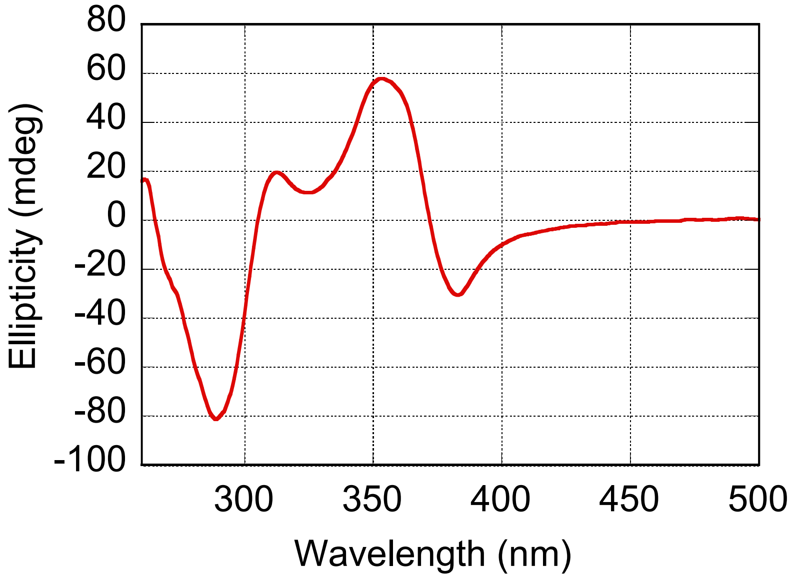

Figure S23. CD spectrum of **1** in 1,1,2-TCE under 200 MPa (16.3×10^{-2} g/L, light path length = 2 mm).

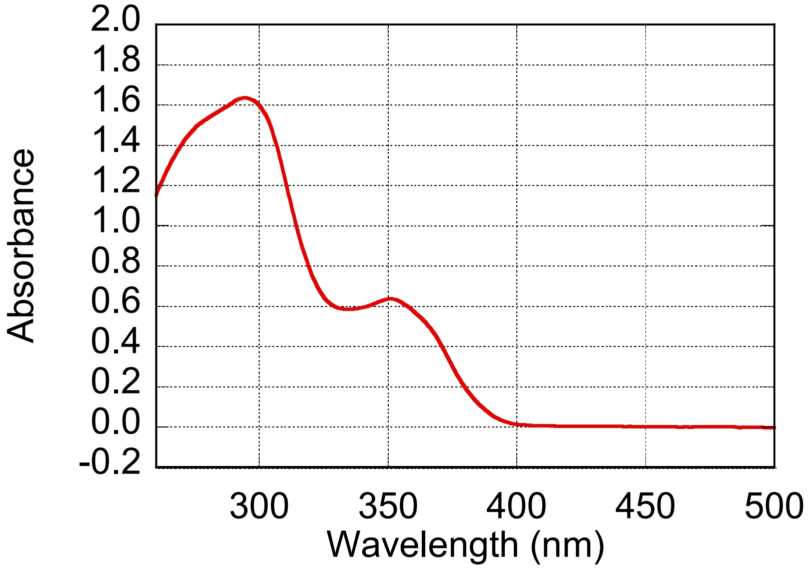

Figure S24. UV-vis absorption of **1** in the 80/20 mixture of $CHCl_3$/1,1,2-TCE under 0.1 MPa (14.5×10^{-2} g/L, light path length = 2 mm).

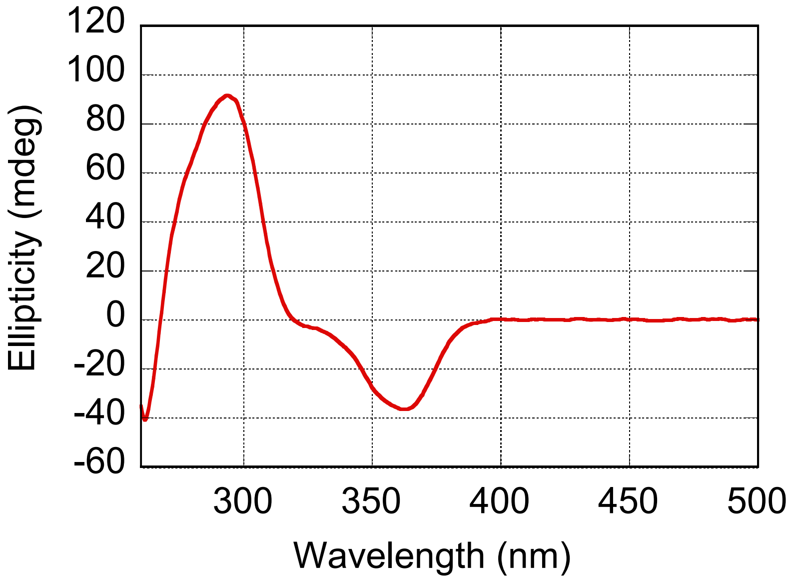

Figure S25. CD spectrum of **1** in the 80/20 mixture of $CHCl_3$/1,1,2-TCE under 0.1 MPa (14.5×10^{-2} g/L, light path length = 2 mm).

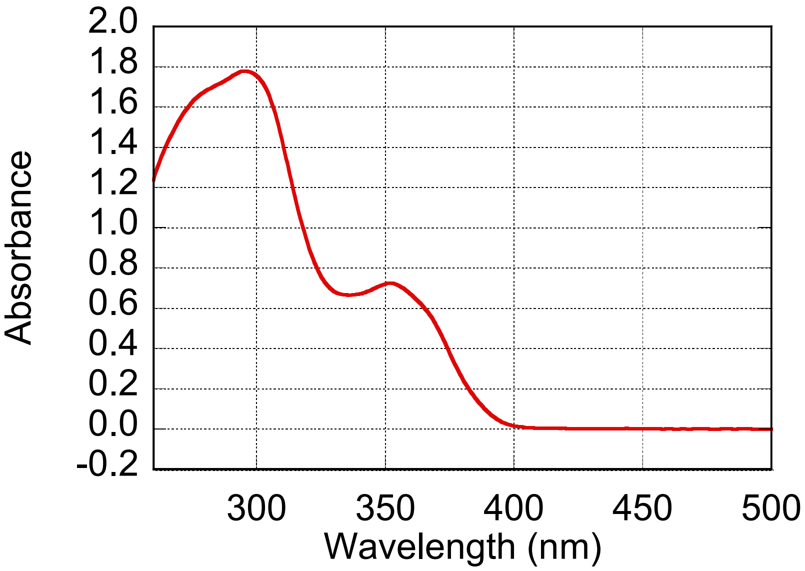

Figure S26. UV-vis absorption of **1** in the 80/20 mixture of $CHCl_3$/1,1,2-TCE under 200 MPa (14.5×10^{-2} g/L, light path length = 2 mm).

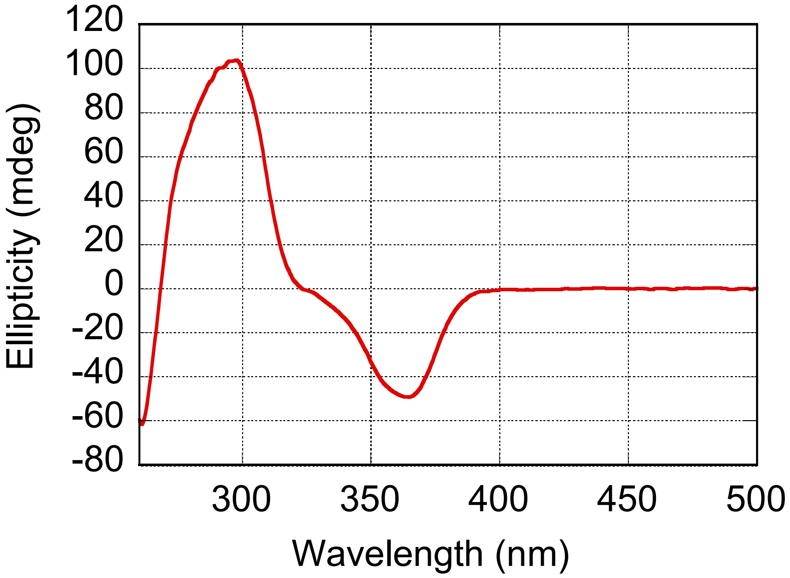

Figure S27. CD spectrum of **1** in the 80/20 mixture of $CHCl_3$/1,1,2-TCE under 200 MPa (14.5×10^{-2} g/L, light path length = 2 mm).

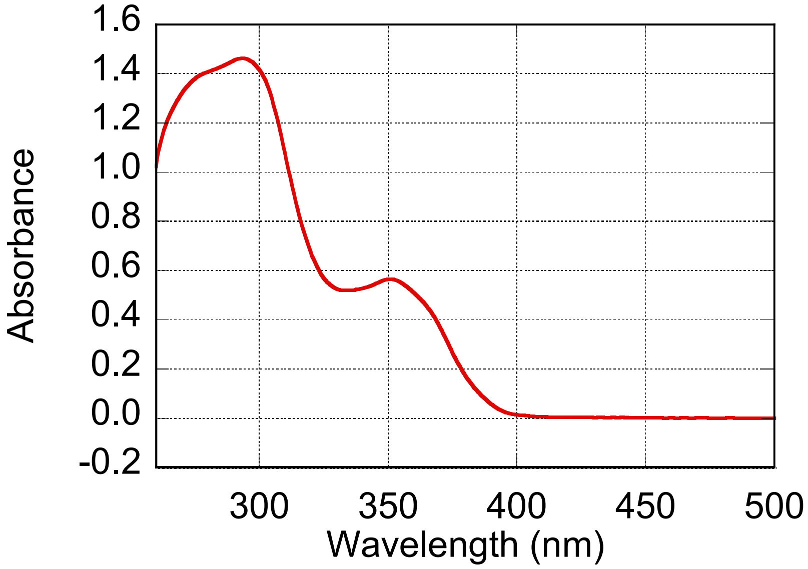

Figure S28. UV-vis absorption of **1** in the 60/40 mixture of $CHCl_3$/1,1,2-TCE under 0.1 MPa (14.5×10^{-2} g/L, light path length = 2 mm).

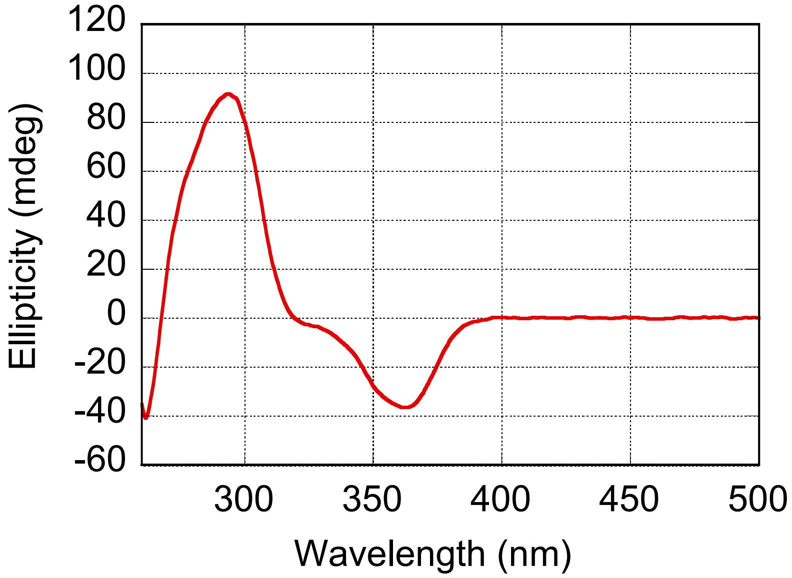

Figure S29. CD spectrum of **1** in the 60/40 mixture of $CHCl_3$/1,1,2-TCE under 0.1 MPa (14.5×10^{-2} g/L, light path length = 2 mm).

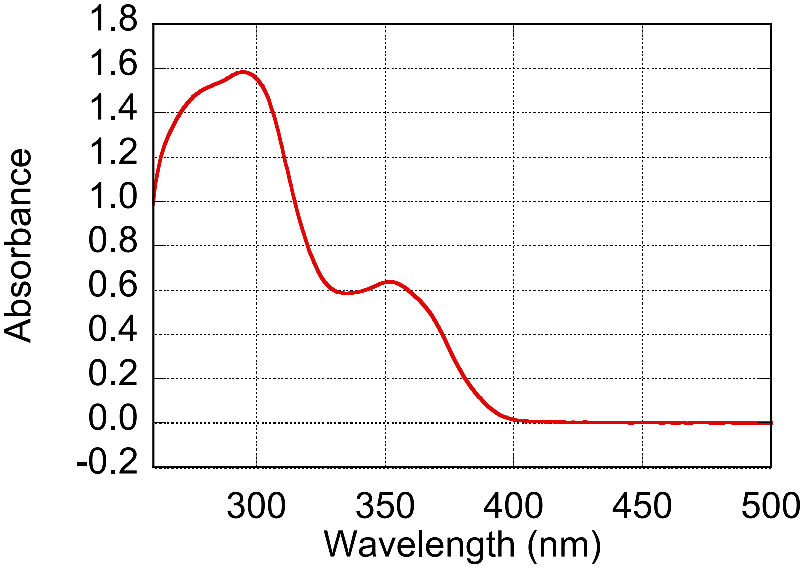

Figure S30. UV-vis absorption of **1** in the 60/40 mixture of $CHCl_3$/1,1,2-TCE under 200 MPa (14.5×10^{-2} g/L, light path length = 2 mm).

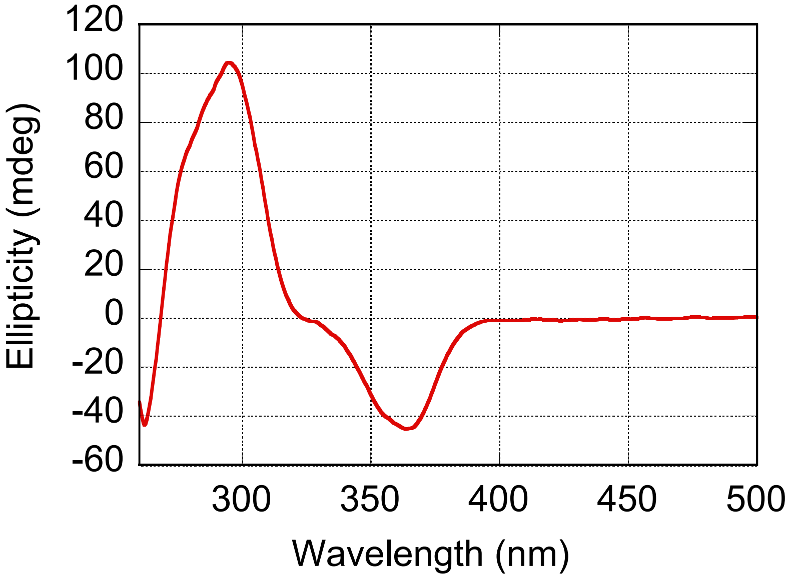

Figure S31. CD spectrum of **1** in the 60/40 mixture of $CHCl_3$/1,1,2-TCE under 200 MPa (14.5×10^{-2} g/L, light path length = 2 mm).

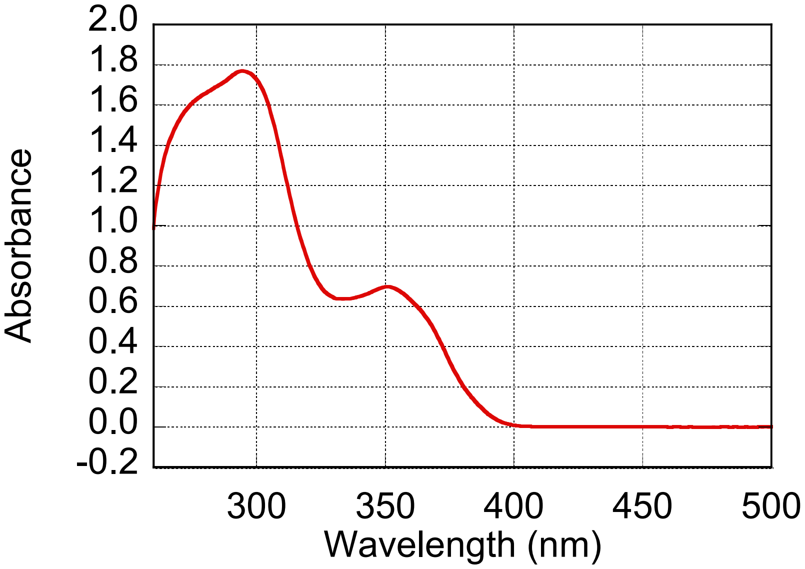

Figure S32. UV-vis absorption of **1** in the 50/50 mixture of $CHCl_3$/1,1,2-TCE under 0.1 MPa (14.5×10^{-2} g/L, light path length = 2 mm).

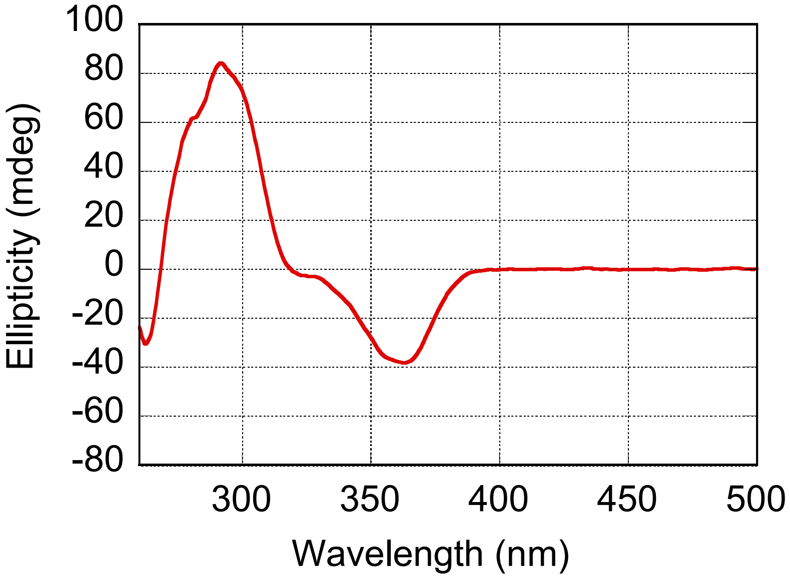

Figure S33. CD spectrum of **1** in the 50/50 mixture of $CHCl_3$/1,1,2-TCE under 0.1 MPa (14.5×10^{-2} g/L, light path length = 2 mm).

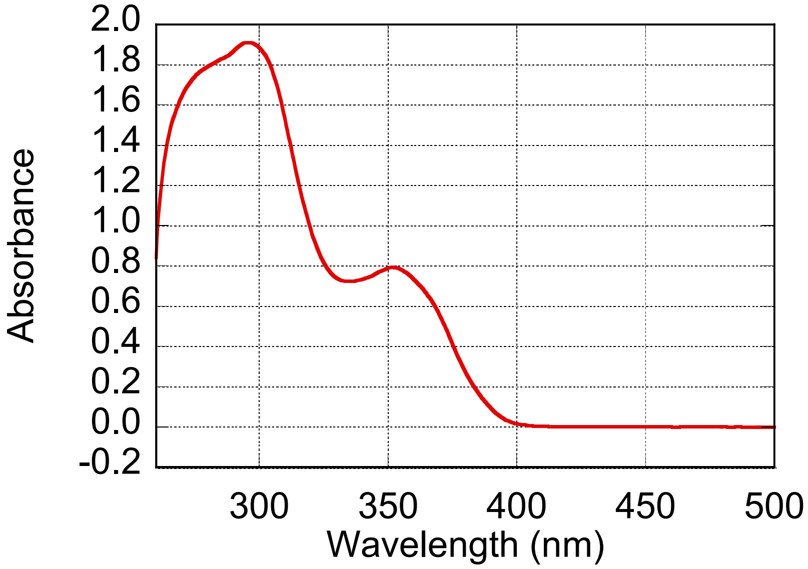

Figure S34. UV-vis absorption of **1** in the 50/50 mixture of $CHCl_3$/1,1,2-TCE under 200 MPa (14.5×10^{-2} g/L, light path length = 2 mm).

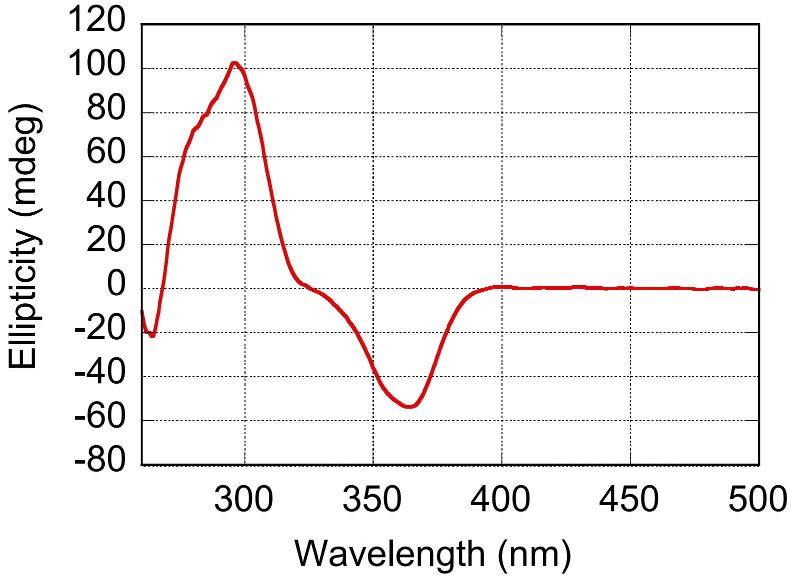

Figure S35. CD spectrum of **1** in the 50/50 mixture of $CHCl_3$/1,1,2-TCE under 200 MPa (14.5×10^{-2} g/L, light path length = 2 mm).

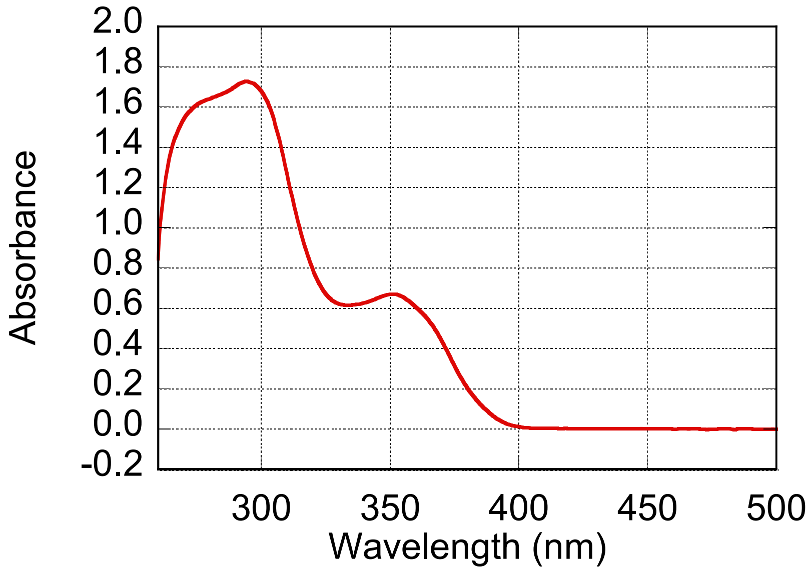

Figure S36. UV-vis absorption of **1** in the 40/60 mixture of $CHCl_3$/1,1,2-TCE under 0.1 MPa (14.5×10^{-2} g/L, light path length = 2 mm).

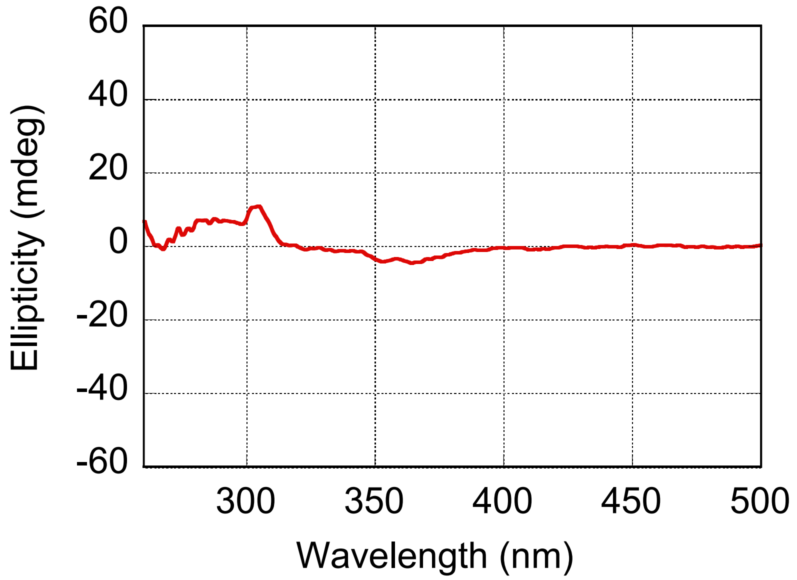

Figure S37. CD spectrum of **1** in the 40/60 mixture of $CHCl_3$/1,1,2-TCE under 0.1 MPa (14.5×10^{-2} g/L, light path length = 2 mm).

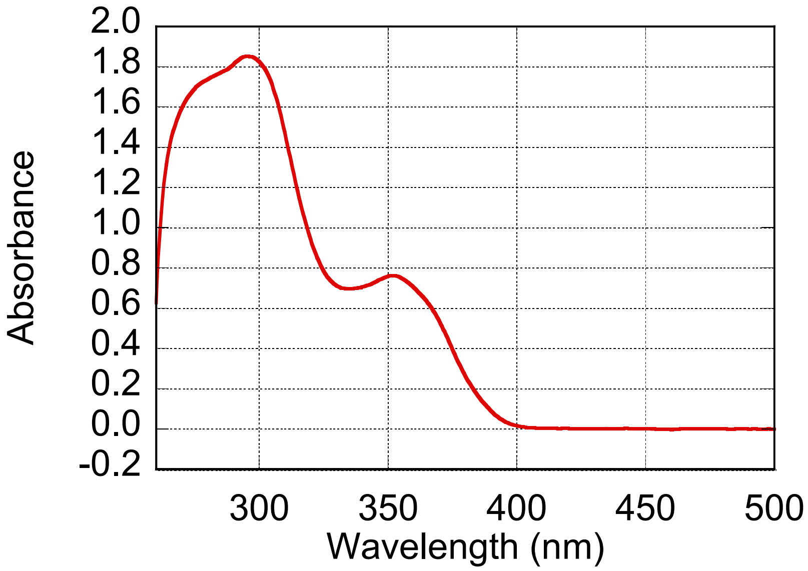

Figure S38. UV-vis absorption of **1** in the 40/60 mixture of $CHCl_3$/1,1,2-TCE under 200 MPa (14.5×10^{-2} g/L, light path length = 2 mm).

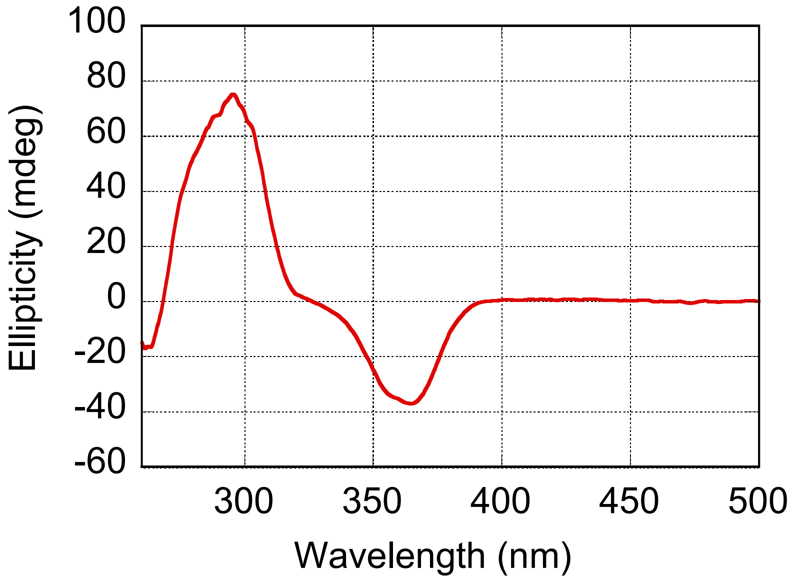

Figure S39. CD spectrum of **1** in the 40/60 mixture of $CHCl_3$/1,1,2-TCE under 200 MPa (14.5×10^{-2} g/L, light path length = 2 mm).

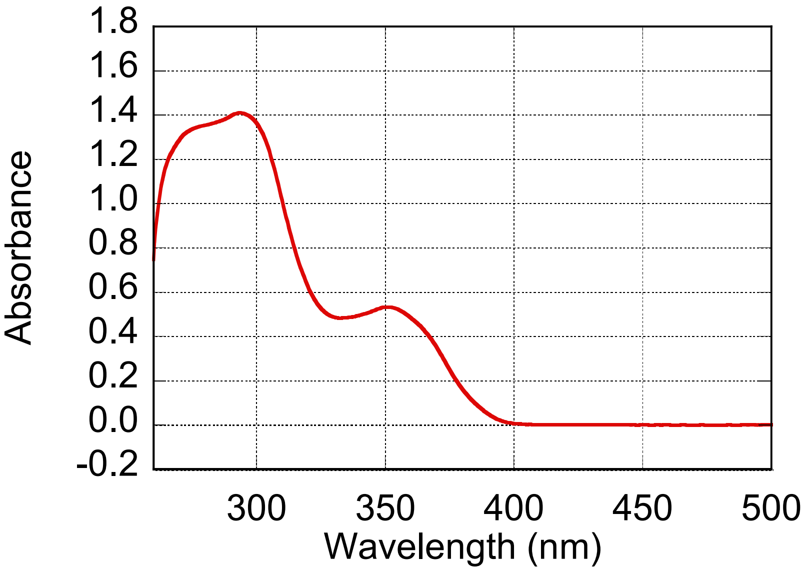

Figure S40. UV-vis absorption of **1** in the 35/65 mixture of $CHCl_3$/1,1,2-TCE under 0.1 MPa (14.5×10^{-2} g/L, light path length = 2 mm).

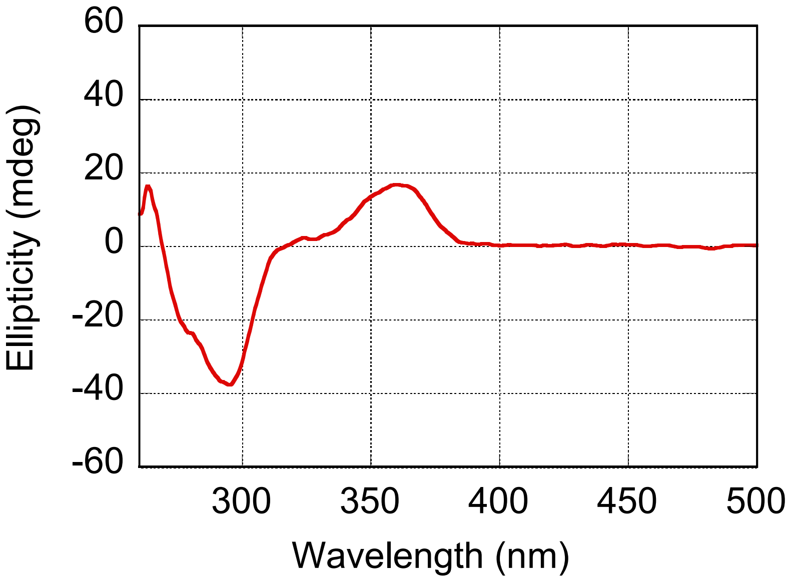

Figure S41. CD spectrum of **1** in the 35/65 mixture of $CHCl_3$/1,1,2-TCE under 0.1 MPa (14.5×10^{-2} g/L, light path length = 2 mm).

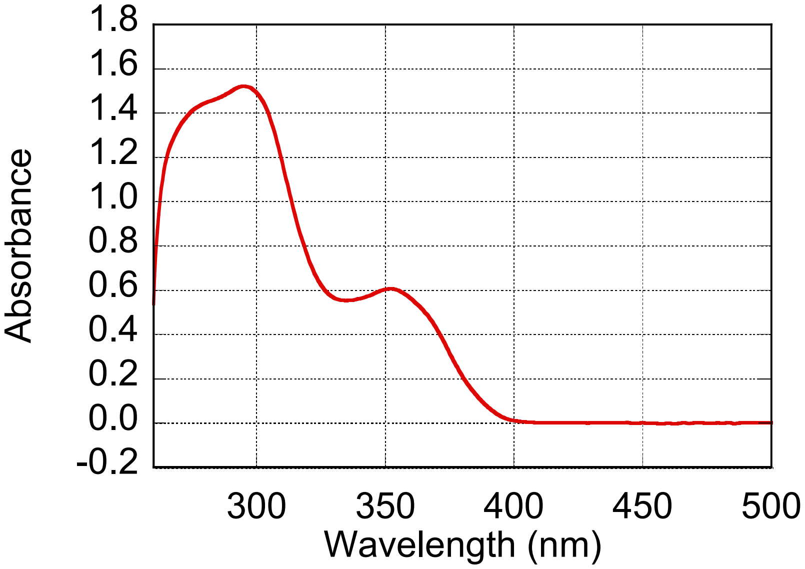

Figure S42. UV-vis absorption of **1** in the 35/65 mixture of $CHCl_3$/1,1,2-TCE under 200 MPa (14.5×10^{-2} g/L, light path length = 2 mm).

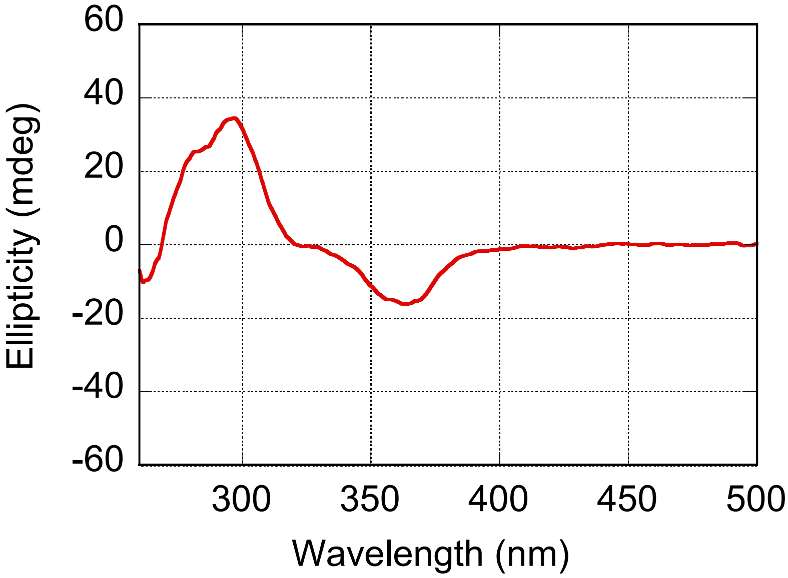

Figure S43. CD spectrum of **1** in the 35/65 mixture of $CHCl_3$/1,1,2-TCE under 200 MPa (14.5×10^{-2} g/L, light path length = 2 mm).

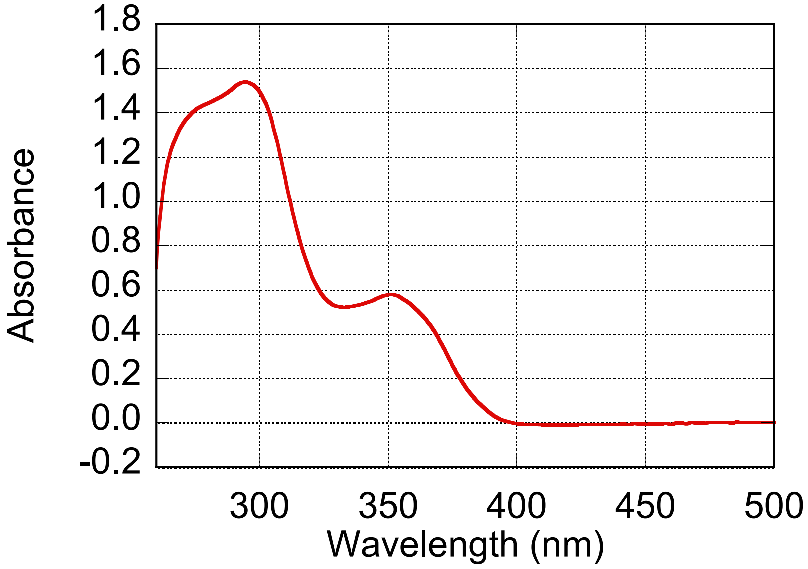

Figure S44. UV-vis absorption of **1** in the 30/70 mixture of $CHCl_3$/1,1,2-TCE under 0.1 MPa (14.5×10^{-2} g/L, light path length = 2 mm).

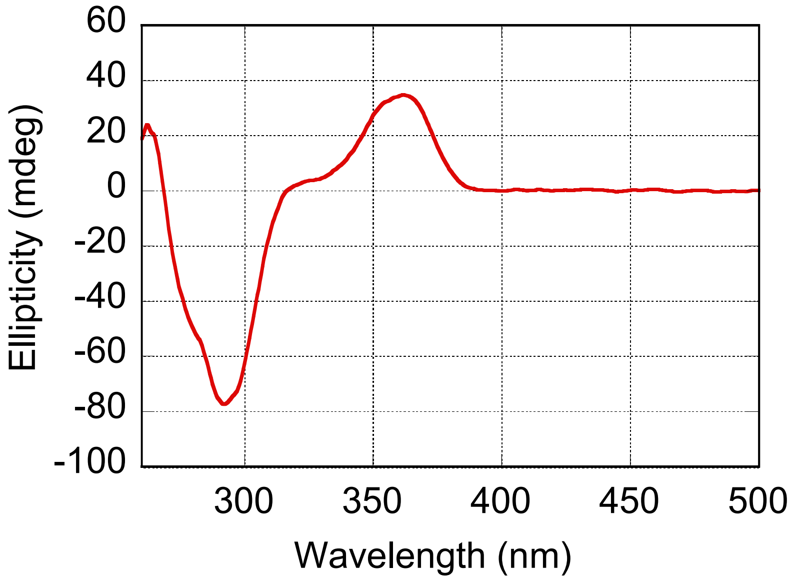

Figure S45. CD spectrum of **1** in the 30/70 mixture of $CHCl_3$/1,1,2-TCE under 0.1 MPa (14.5×10^{-2} g/L, light path length = 2 mm).

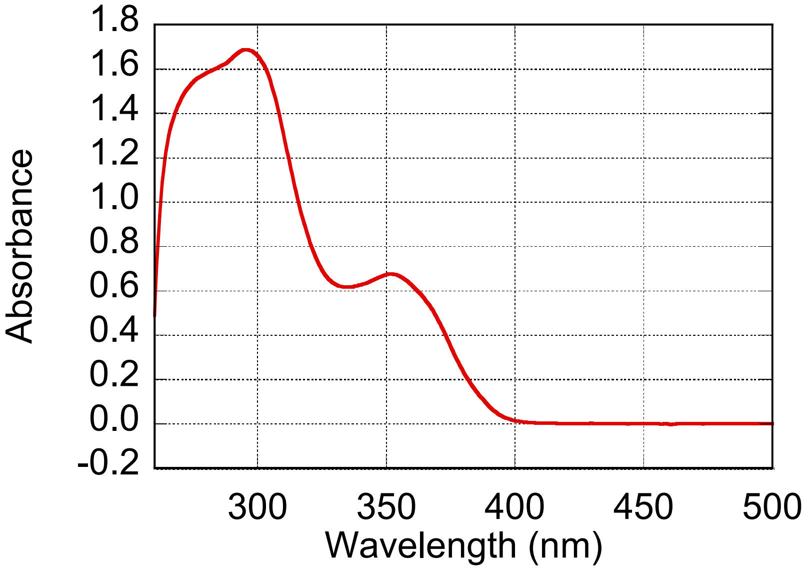

Figure S46. UV-vis absorption of **1** in the 30/70 mixture of $CHCl_3$/1,1,2-TCE under 200 MPa (14.5×10^{-2} g/L, light path length = 2 mm).

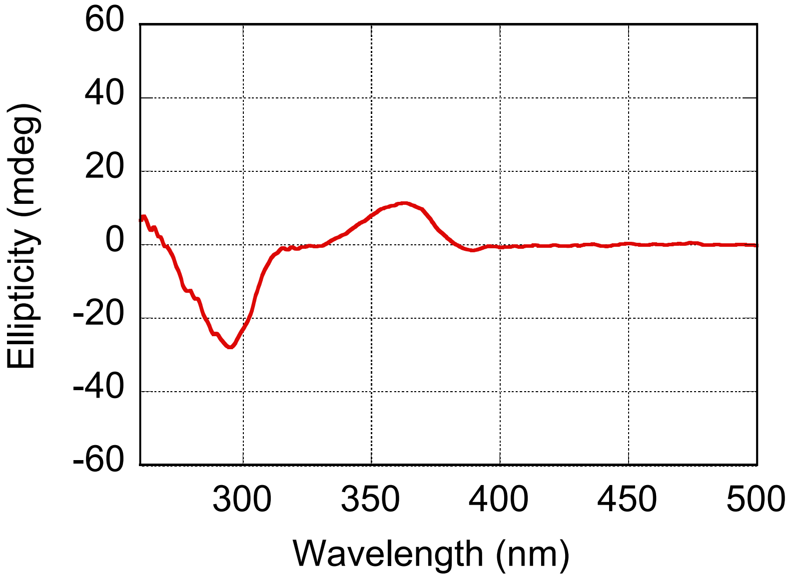

Figure S47. CD spectrum of **1** in the 30/70 mixture of $CHCl_3$/1,1,2-TCE under 200 MPa (14.5×10^{-2} g/L, light path length = 2 mm).

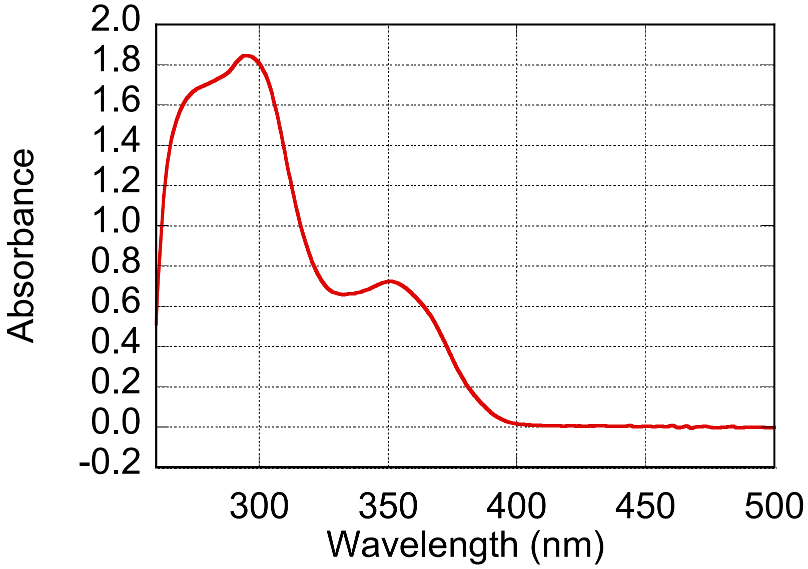

Figure S48. UV-vis absorption of **1** in the 20/80 mixture of $CHCl_3$/1,1,2-TCE under 0.1 MPa (14.5 × 10^{-2} g/L, light path length = 2 mm).

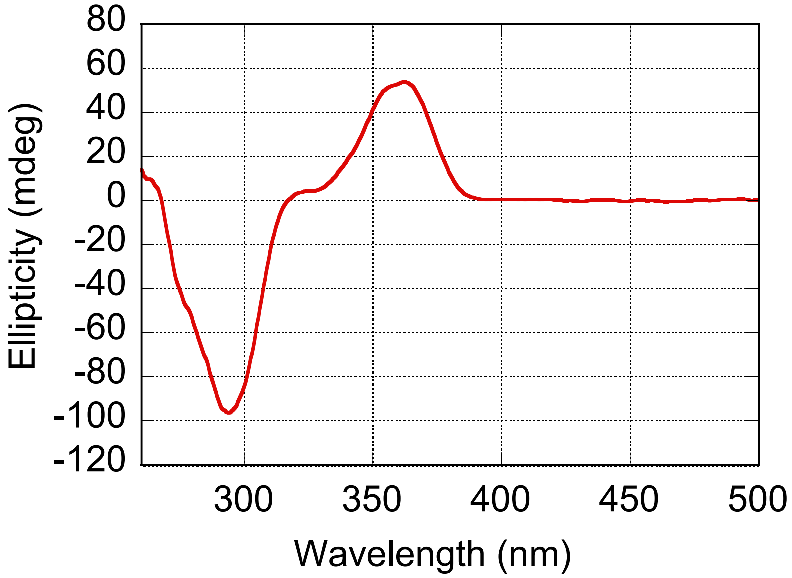

Figure S49. CD spectrum of **1** in the 20/80 mixture of $CHCl_3$/1,1,2-TCE under 0.1 MPa (14.5 × 10^{-2} g/L, light path length = 2 mm).

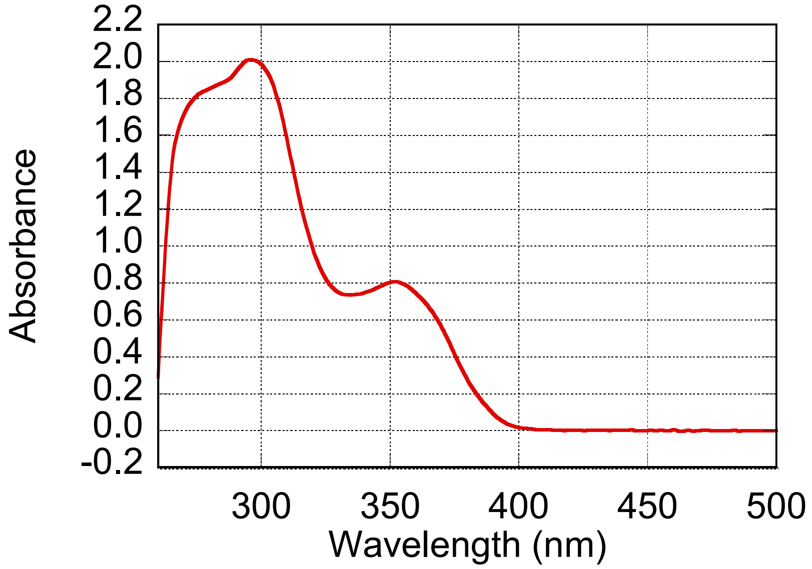

Figure S50. UV-vis absorption of **1** in the 20/80 mixture of $CHCl_3$/1,1,2-TCE under 200 MPa (14.5×10^{-2} g/L, light path length = 2 mm).

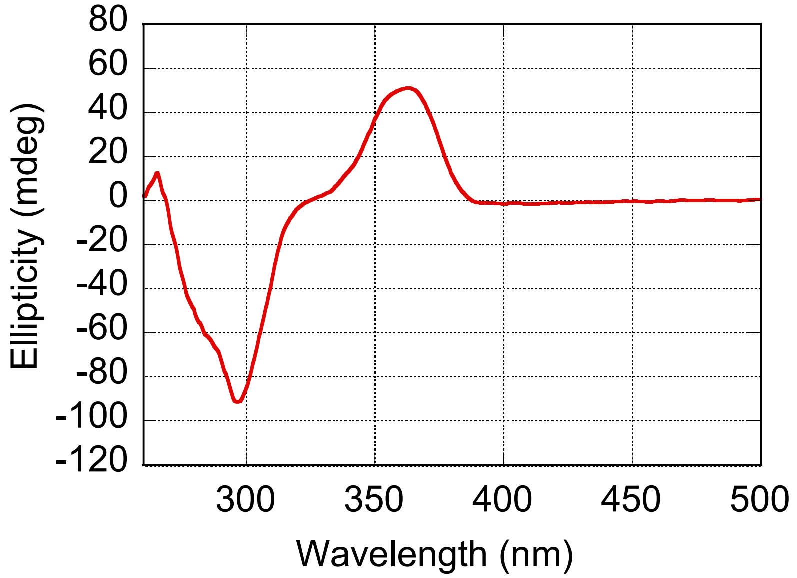

Figure S51. CD spectrum of **1** in the 20/80 mixture of $CHCl_3$/1,1,2-TCE under 200 MPa (14.5×10^{-2} g/L, light path length = 2 mm).

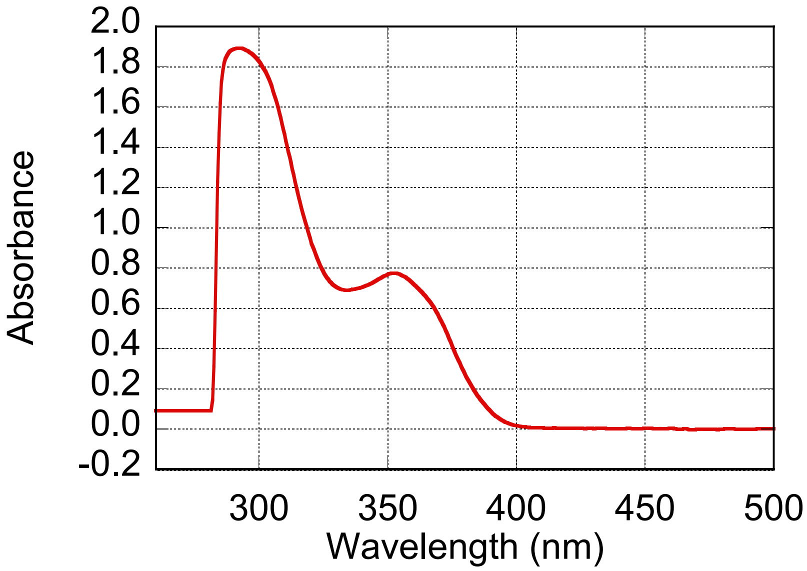

Figure S52. UV-vis absorption of **1** in toluene under 0.1 MPa (15.5×10^{-2} g/L, light path length = 2 mm).

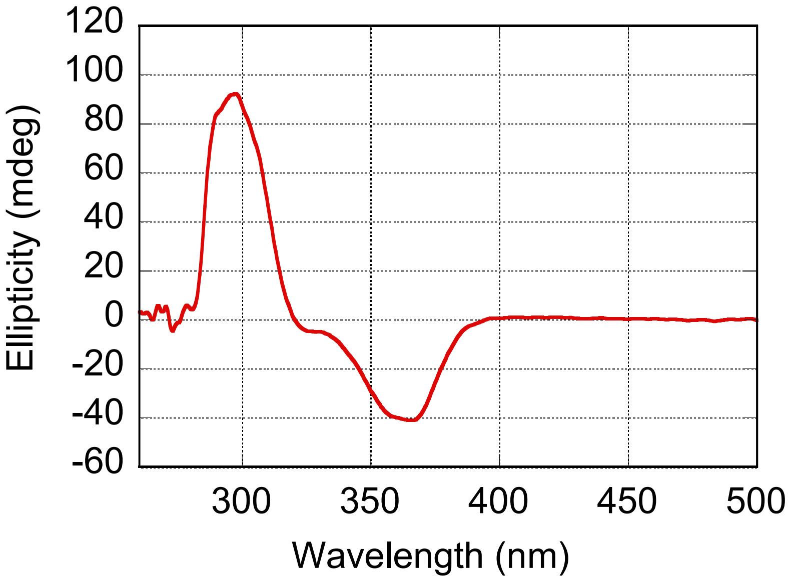

Figure S53. CD spectrum of **1** in toluene under 0.1 MPa (15.5×10^{-2} g/L, light path length = 2 mm).

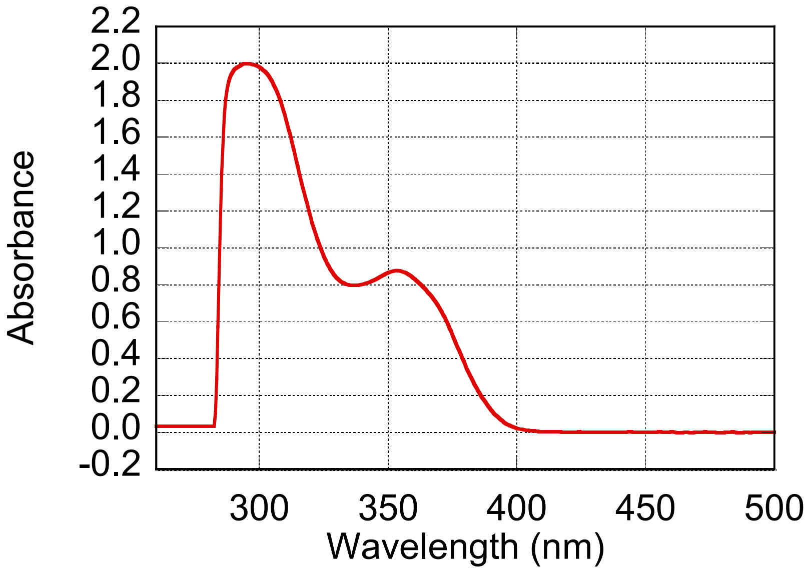

Figure S54. UV-vis absorption of **1** in toluene under 200 MPa (15.5×10^{-2} g/L, light path length = 2 mm).

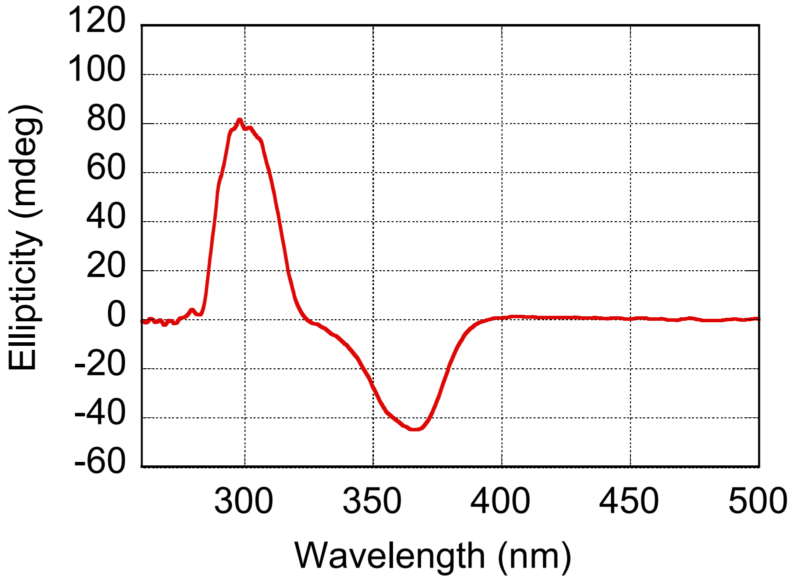

Figure S55. CD spectrum of **1** in toluene under 200 MPa (15.5×10^{-2} g/L, light path length = 2 mm).

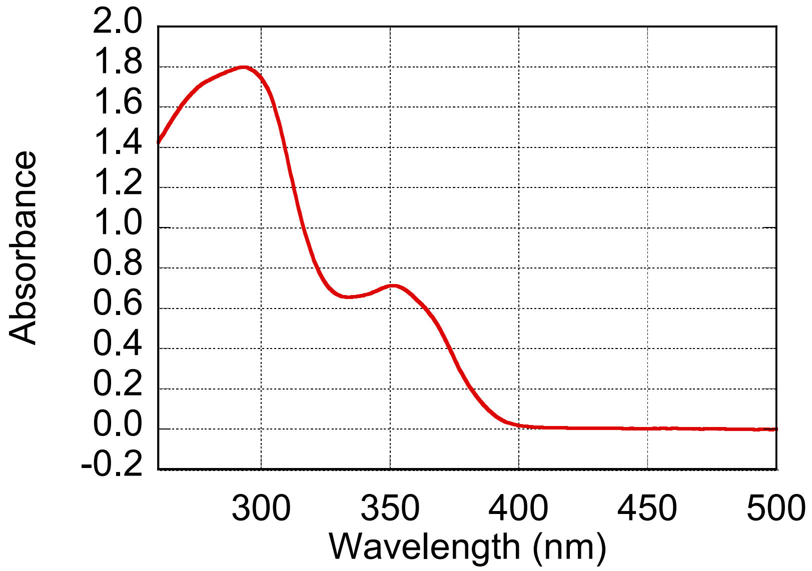

Figure S56. UV-vis absorption of **1** in CH_2Cl_2 under 0.1 MPa (14.6×10^{-2} g/L, light path length = 2 mm).

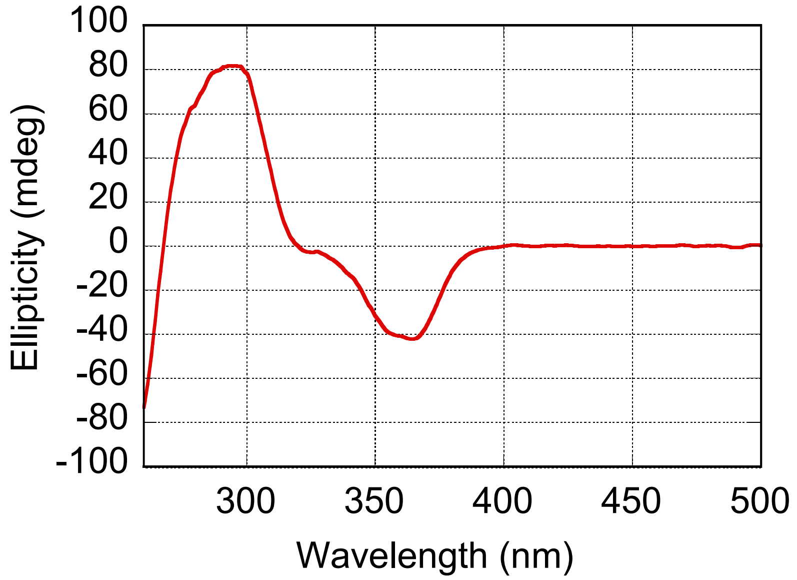

Figure S57. CD spectrum of **1** in CH_2Cl_2 under 0.1 MPa (14.6×10^{-2} g/L, light path length = 2 mm).

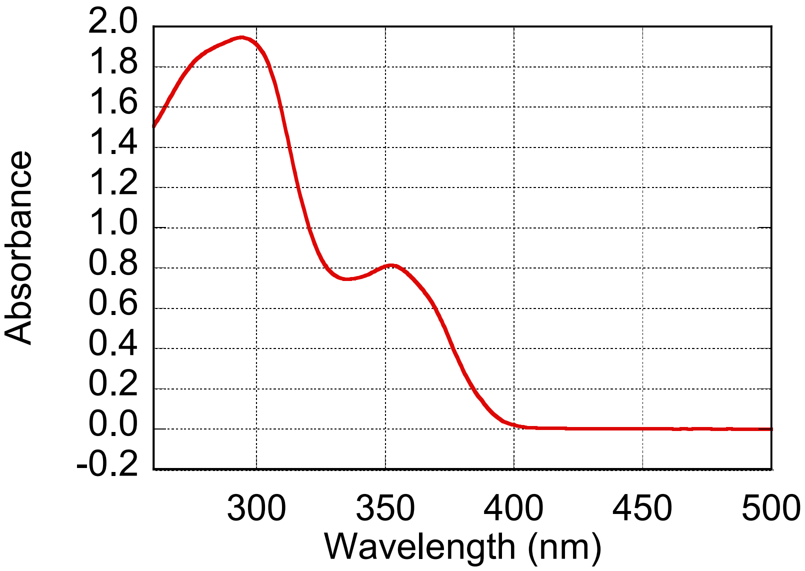

Figure S58. UV-vis absorption of **1** in CH_2Cl_2 under 200 MPa (14.6×10^{-2} g/L, light path length = 2 mm).

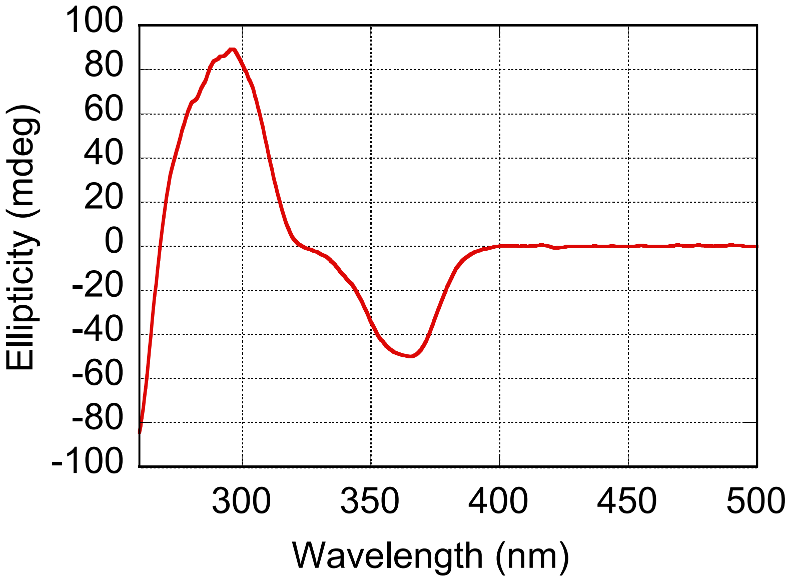

Figure S59. CD spectrum of **1** in CH_2Cl_2 under 200 MPa (14.6×10^{-2} g/L, light path length = 2 mm).

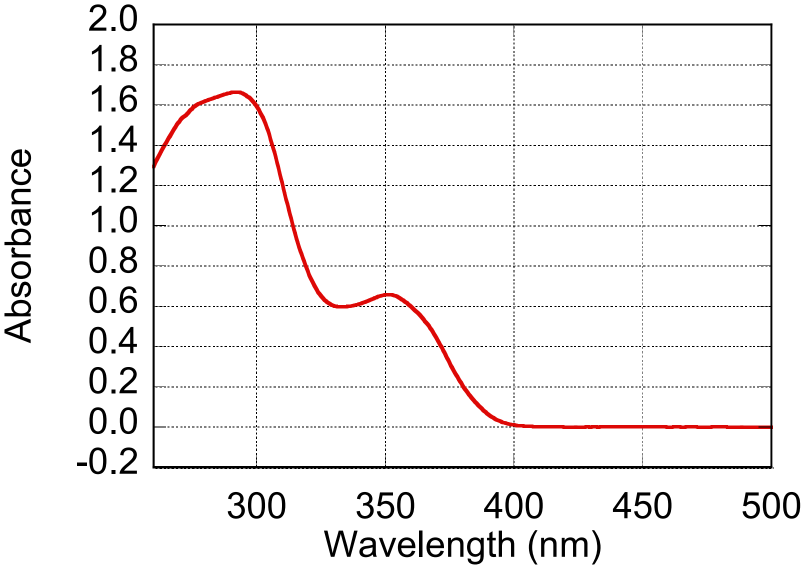

Figure S60. UV-vis absorption of **1** in 1,1,1-TCE under 0.1 MPa (14.0×10^{-2} g/L, light path length = 2 mm).

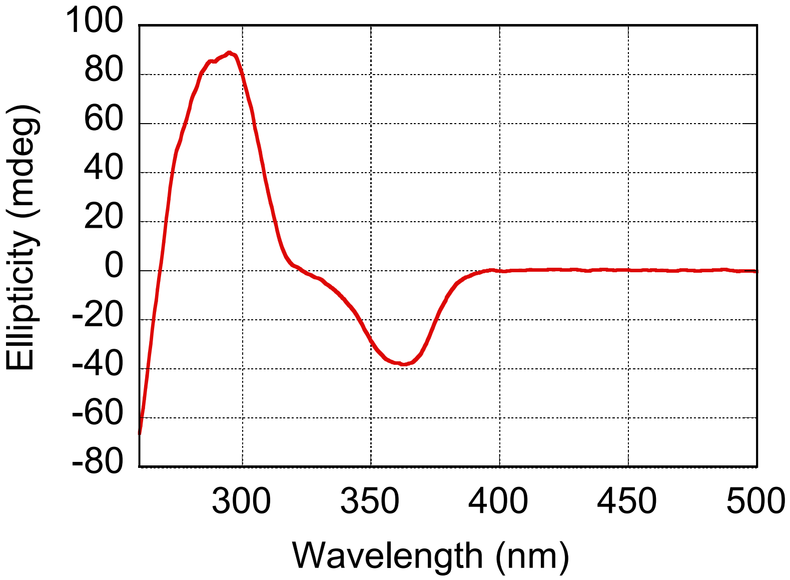

Figure S61. CD spectrum of **1** in 1,1,1-TCE under 0.1 MPa (14.0×10^{-2} g/L, light path length = 2 mm).

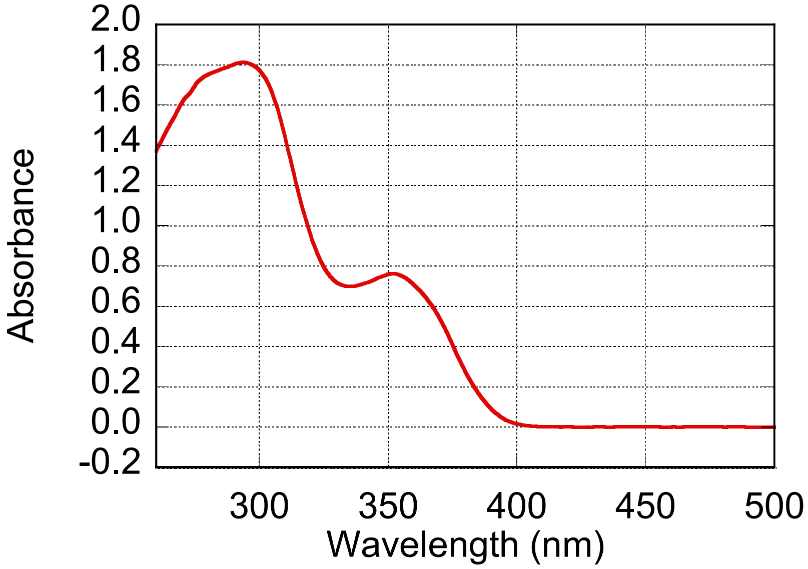

Figure S62. UV-vis absorption of **1** in 1,1,1-TCE under 200 MPa

(14.0×10^{-2} g/L, light path length = 2 mm).

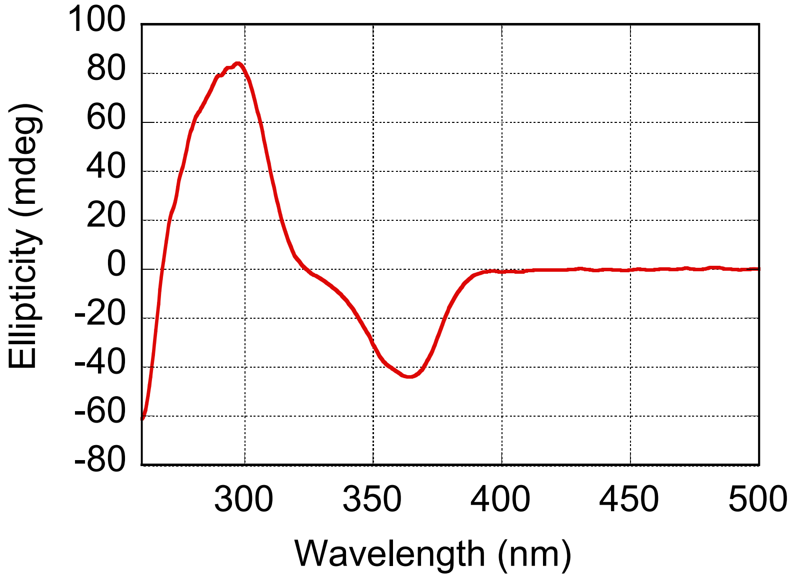

Figure S63. CD spectrum of **1** in 1,1,1-TCE under 200 MPa

(14.0×10^{-2} g/L, light path length = 2 mm).

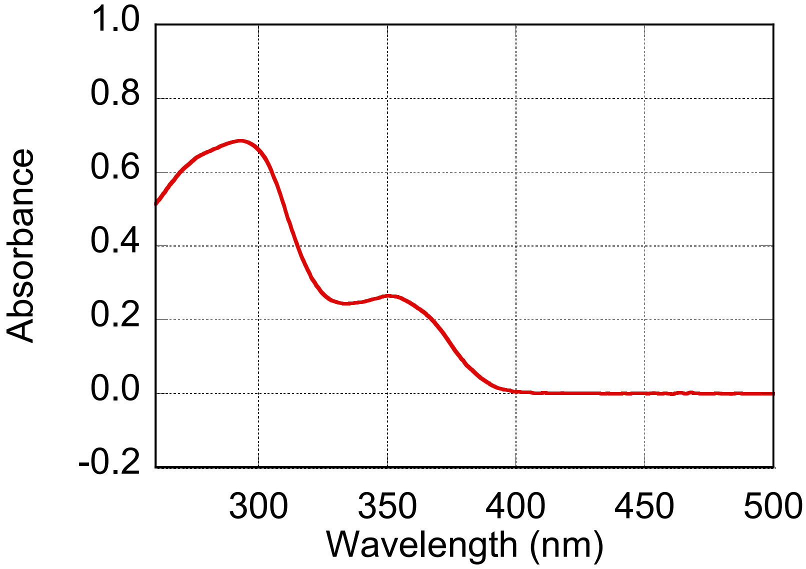

Figure S64. UV-vis absorption of **1** in THF under 0.1 MPa (15.9×10^{-2} g/L, light path length = 2 mm).

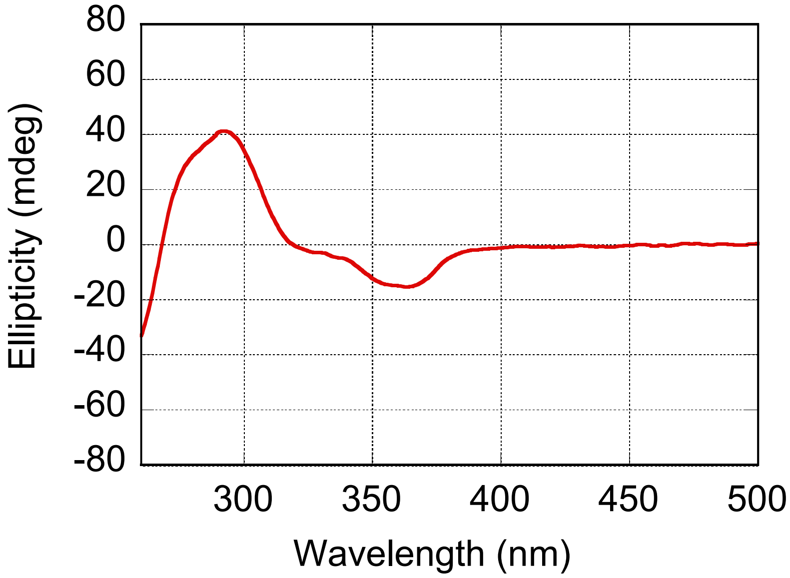

Figure S65. CD spectrum of **1** in THF under 0.1 MPa (15.9×10^{-2} g/L, light path length = 2 mm).

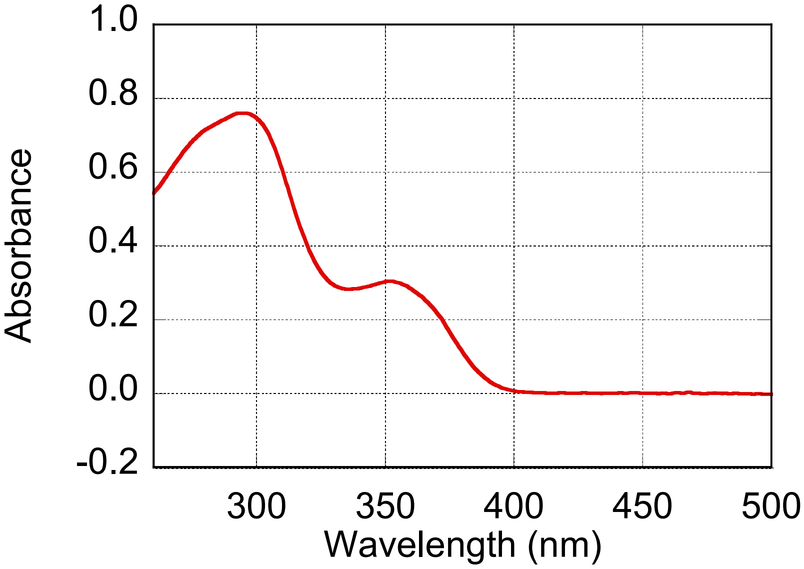

Figure S66. UV-vis absorption of **1** in THF under 200 MPa

(15.9×10^{-2} g/L, light path length = 2 mm).

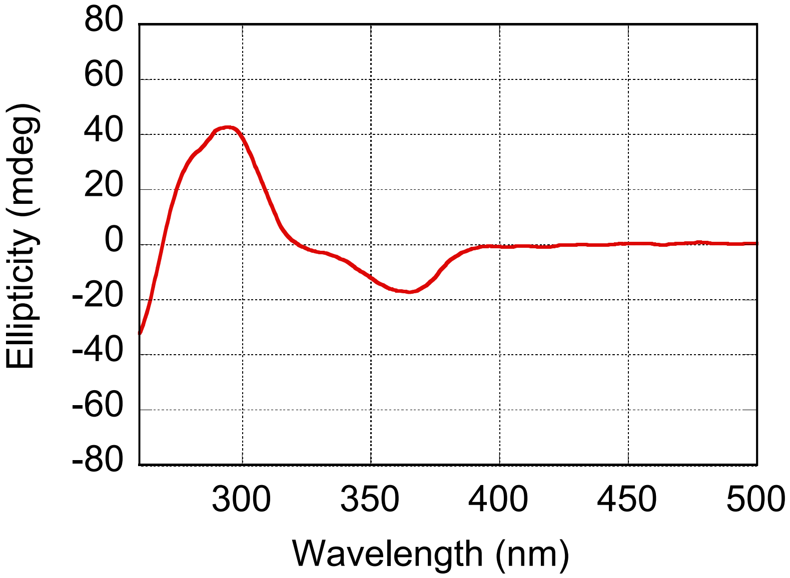

Figure S67. CD spectrum of **1** in THF under 200 MPa

(15.9×10^{-2} g/L, light path length = 2 mm).

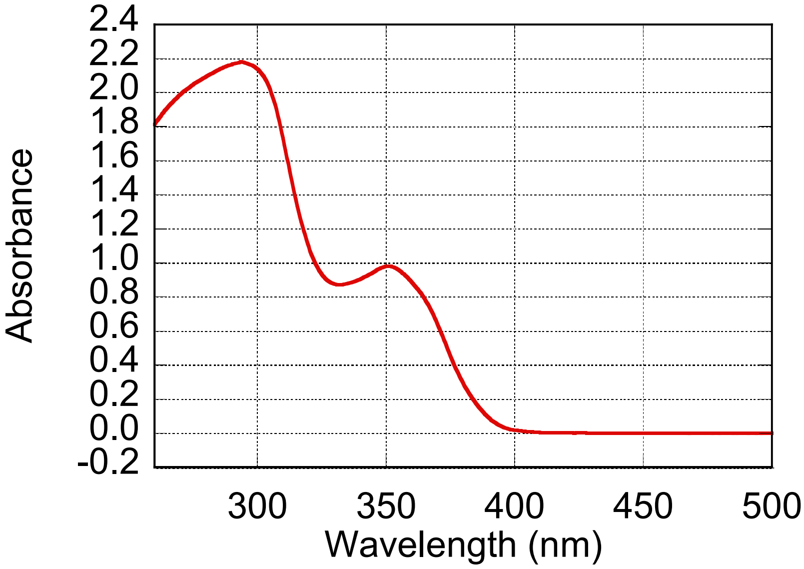

Figure S68. UV-vis absorption of **1** in 1-BuCl under 0.1 MPa (14.3×10^{-2} g/L, light path length = 2 mm).

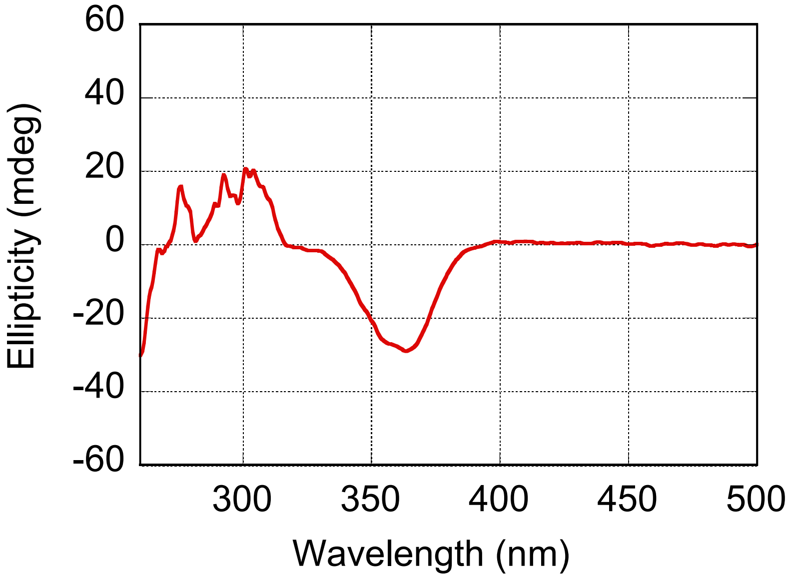

Figure S69. CD spectrum of **1** in 1-BuCl under 0.1 MPa (14.3×10^{-2} g/L, light path length = 2 mm).

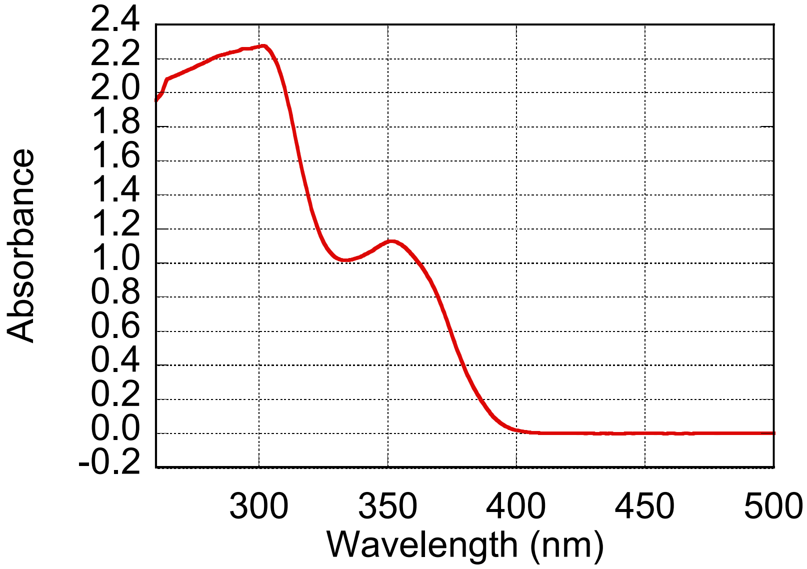

Figure S70. UV-vis absorption of **1** in 1-BuCl under 200 MPa (14.3×10^{-2} g/L, light path length = 2 mm).

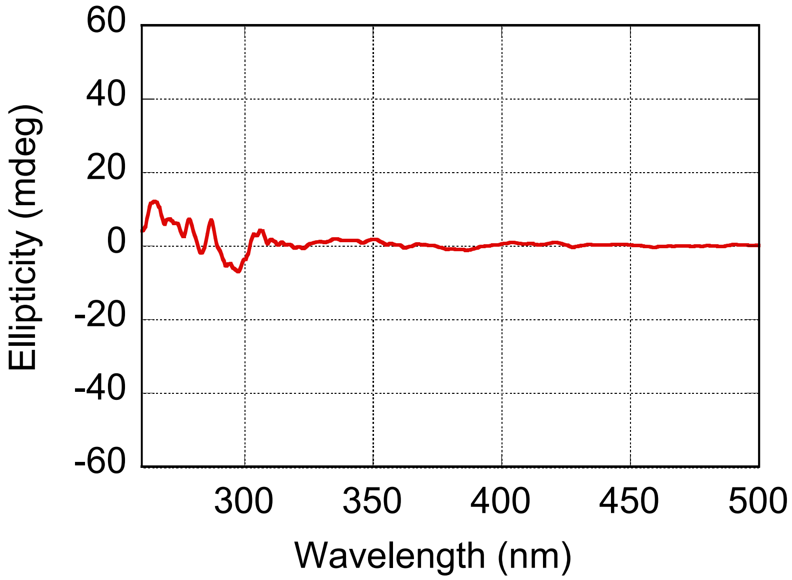

Figure S71. CD spectrum of **1** in 1-BuCl under 200 MPa (14.3×10^{-2} g/L, light path length = 2 mm).

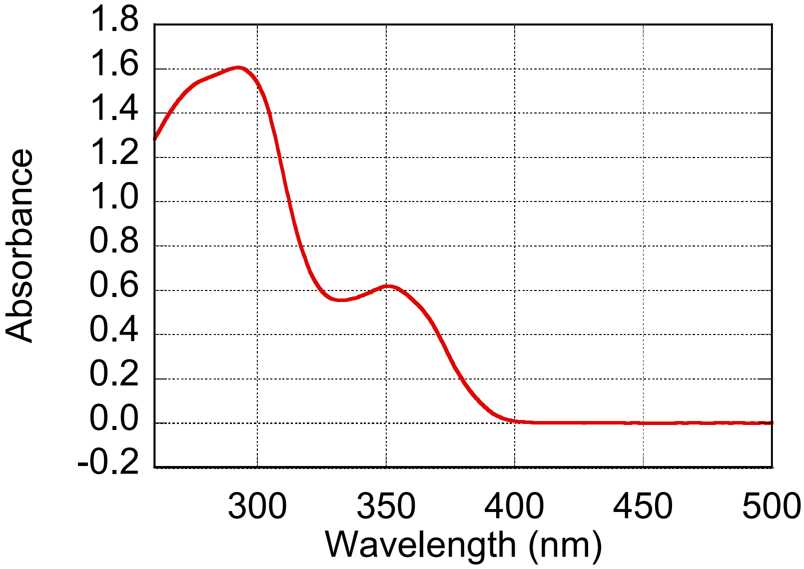

Figure S72. UV-vis absorption of **1** in 1-BuCN under 0.1 MPa (12.8×10^{-2} g/L, light path length = 2 mm).

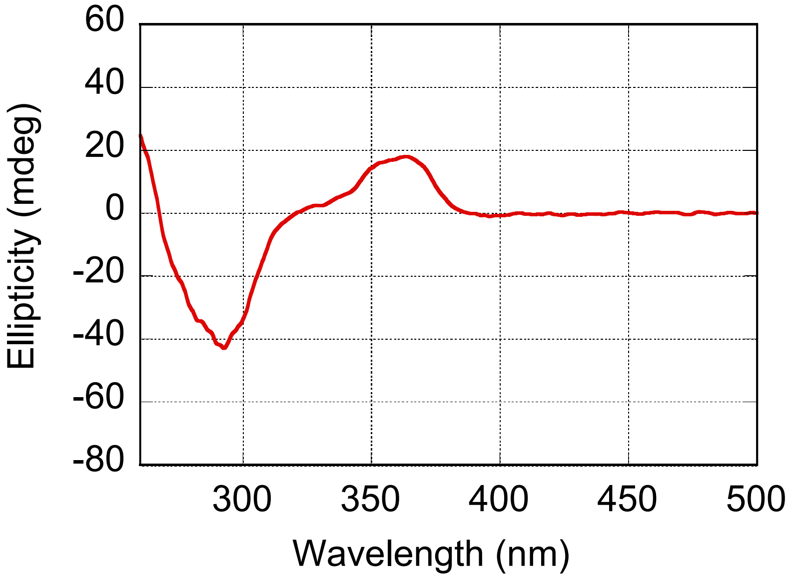

Figure S73. CD spectrum of **1** in 1-BuCN under 0.1 MPa (12.8×10^{-2} g/L, light path length = 2 mm).

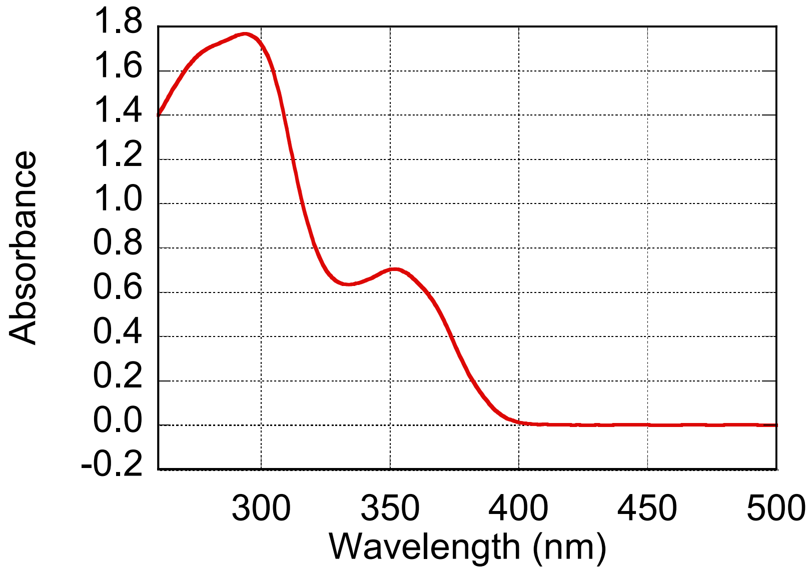

Figure S74. UV-vis absorption of **1** in 1-BuCN under 200 MPa (12.8×10^{-2} g/L, light path length = 2 mm).

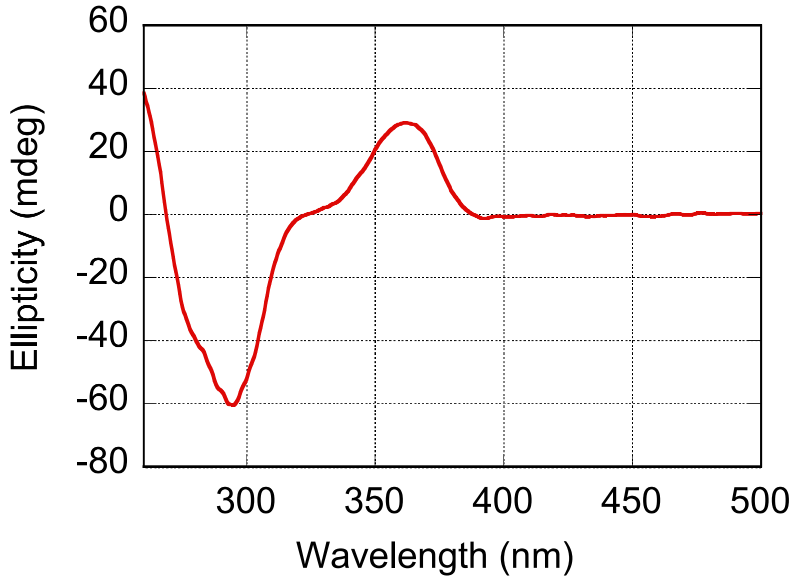

Figure S75. CD spectrum of **1** in 1-BuCN under 200 MPa (12.8×10^{-2} g/L, light path length = 2 mm).

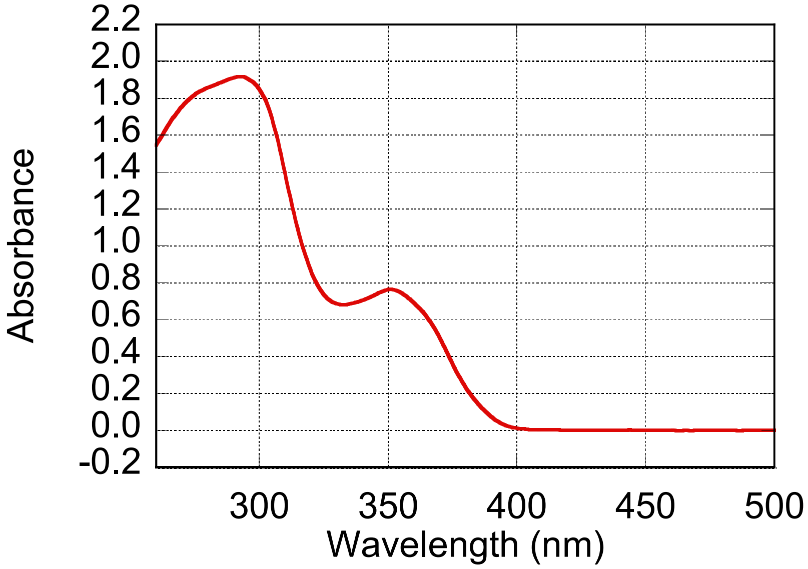

Figure S76. UV-vis absorption of **1** in 1,2-DCE under 0.1 MPa (14.5×10^{-2} g/L, light path length = 2 mm).

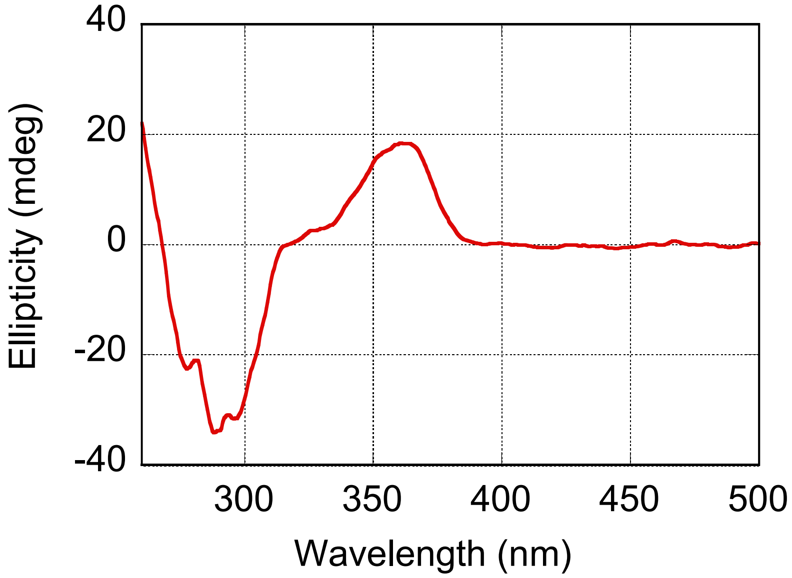

Figure S77. CD spectrum of **1** in 1,2-DCE under 0.1 MPa (14.5×10^{-2} g/L, light path length = 2 mm).

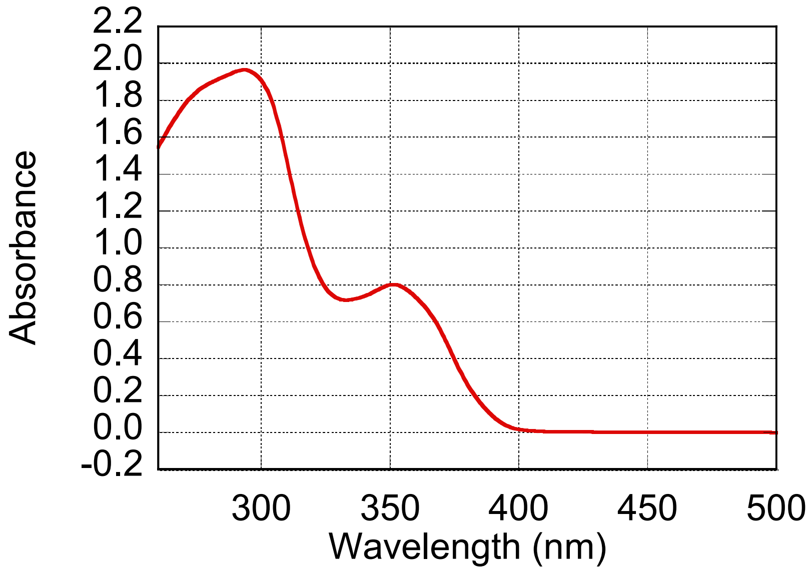

Figure S78. UV-vis absorption of **1** in 1,2-DCE under 50 MPa (14.5×10^{-2} g/L, light path length = 2 mm).

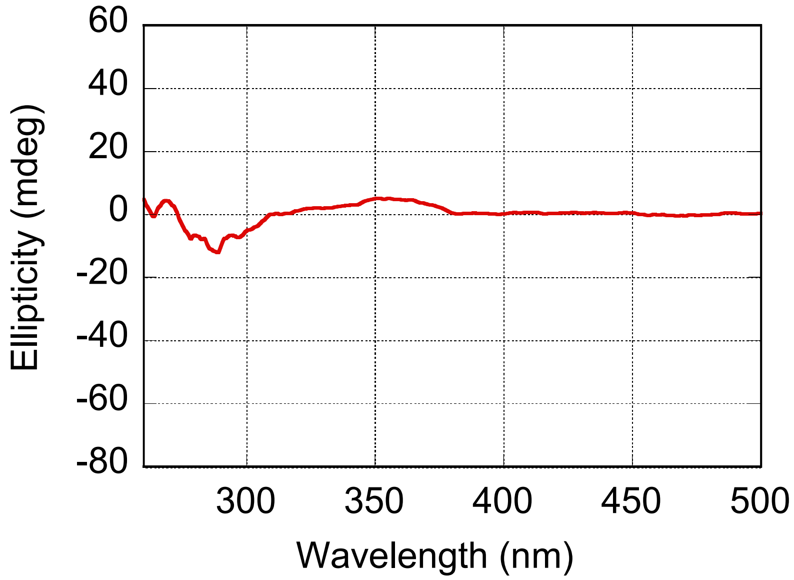

Figure S79. CD spectrum of **1** in 1,2-DCE under 50 MPa (14.5×10^{-2} g/L, light path length = 2 mm).

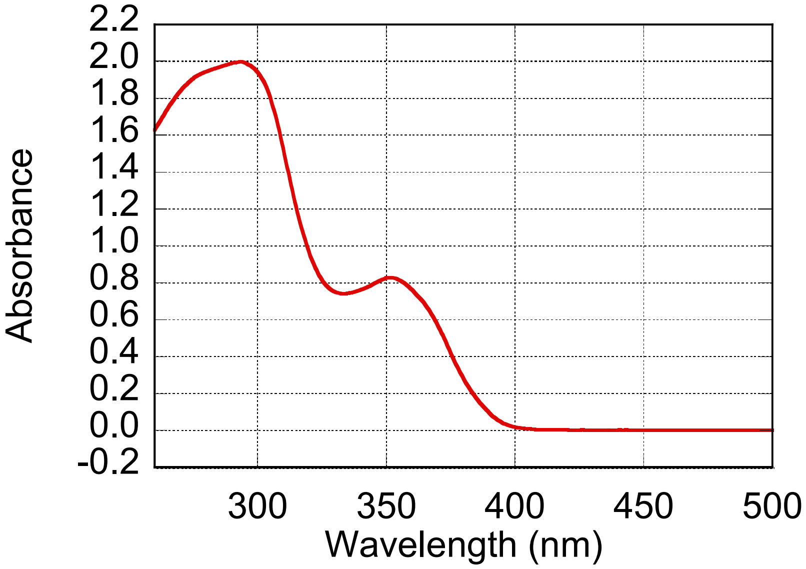

Figure S80. UV-vis absorption of **1** in 1,2-DCE under 100 MPa (14.5×10^{-2} g/L, light path length = 2 mm).

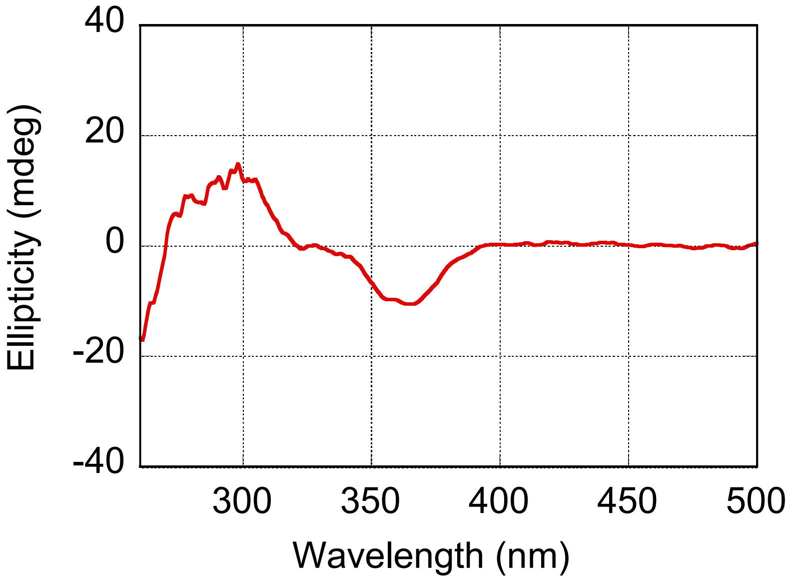

Figure S81. CD spectrum of **1** in 1,2-DCE under 100 MPa (14.5×10^{-2} g/L, light path length = 2 mm).

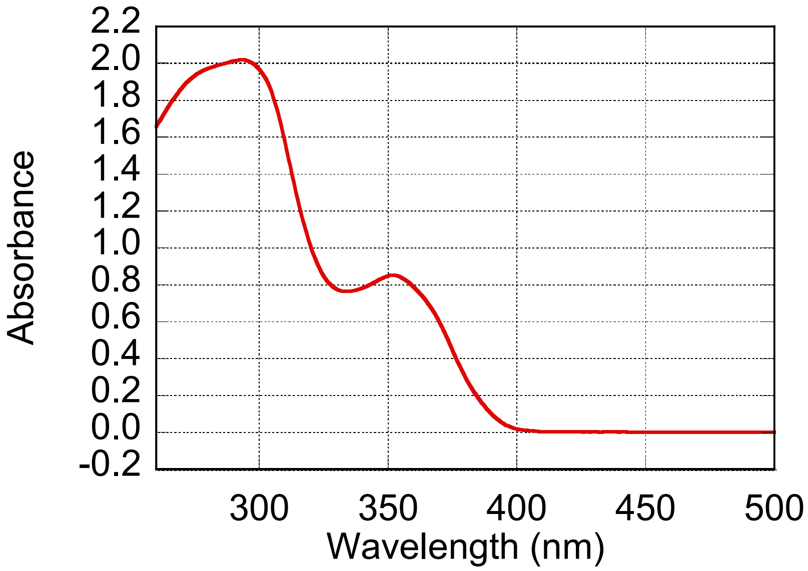

Figure S82. UV-vis absorption of **1** in 1,2-DCE under 150 MPa (14.5×10^{-2} g/L, light path length = 2 mm)

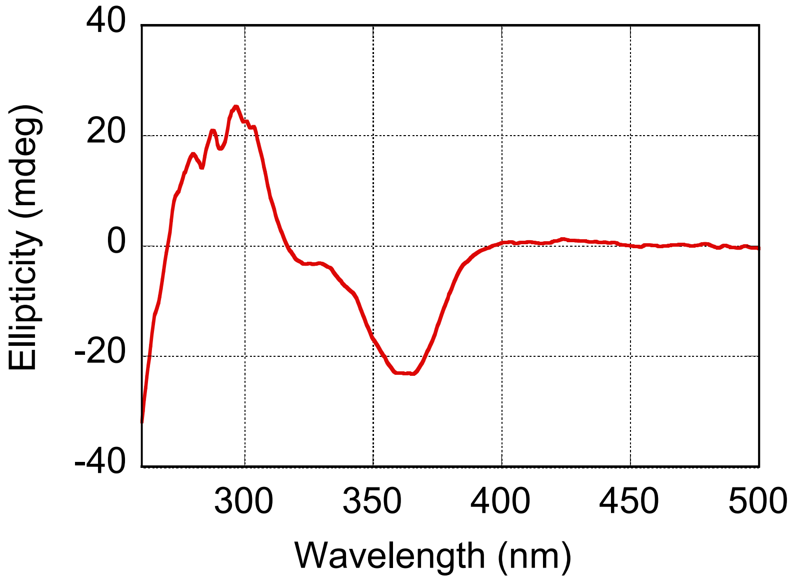

Figure S83. CD spectrum of **1** in 1,2-DCE under 150 MPa (14.5×10^{-2} g/L, light path length = 2 mm).

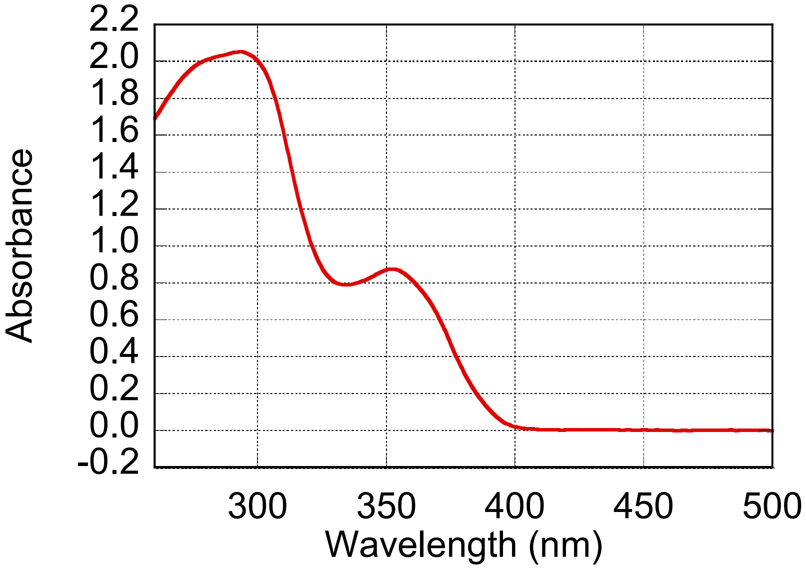

Figure S84. UV-vis absorption of **1** in 1,2-DCE under 200 MPa

(14.5 × 10^{-2} g/L, light path length = 2 mm).

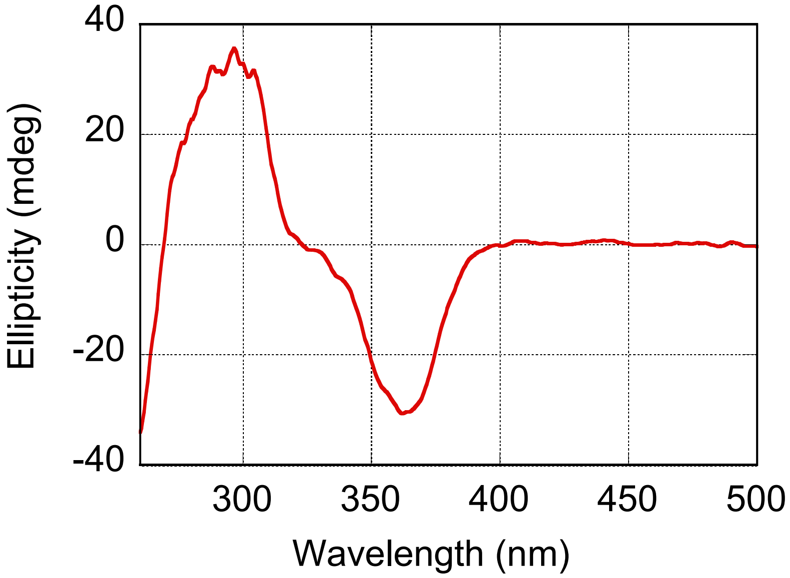

Figure S85. CD spectrum of **1** in 1,2-DCE under 200 MPa

(14.5 × 10^{-2} g/L, light path length = 2 mm).

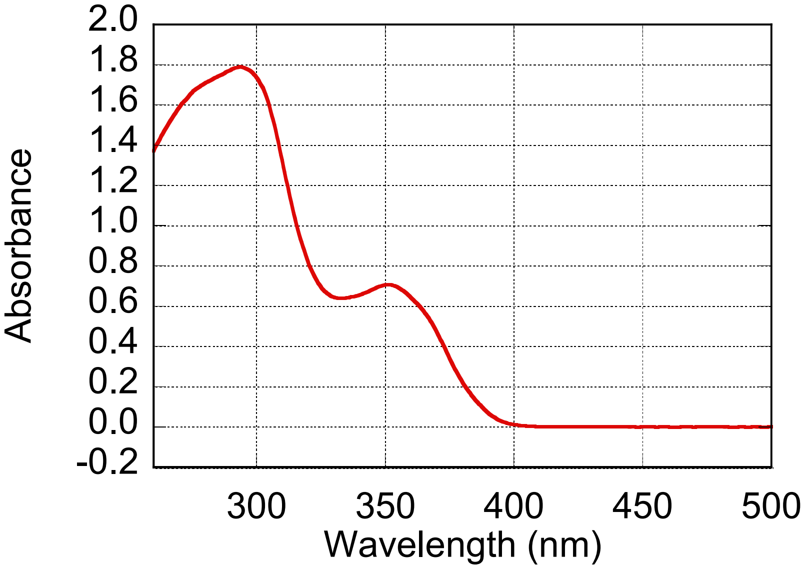

Figure S86. UV-vis absorption of **1** in 1,3-dichloropropane under 0.1 MPa (15.1×10^{-2} g/L, light path length = 2 mm).

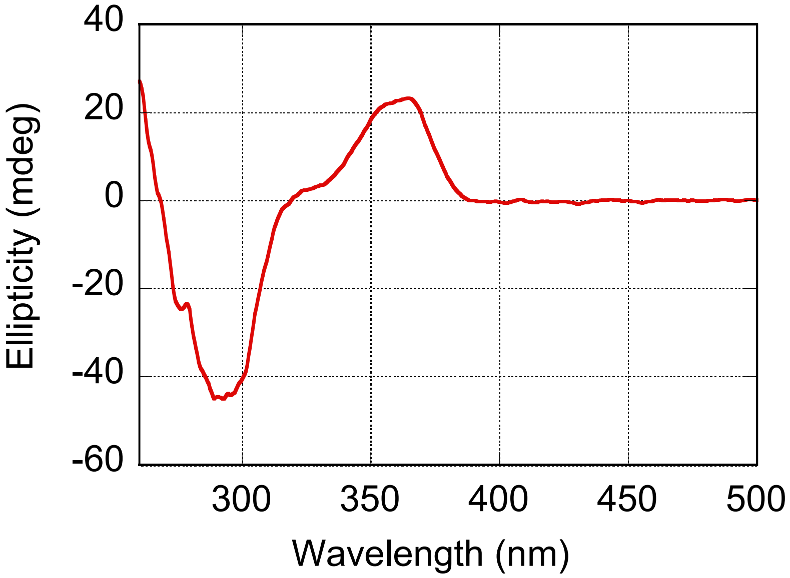

Figure S87. CD spectrum of **1** in 1,3-dichloropropane under 0.1 MPa (15.1×10^{-2} g/L, light path length = 2 mm).

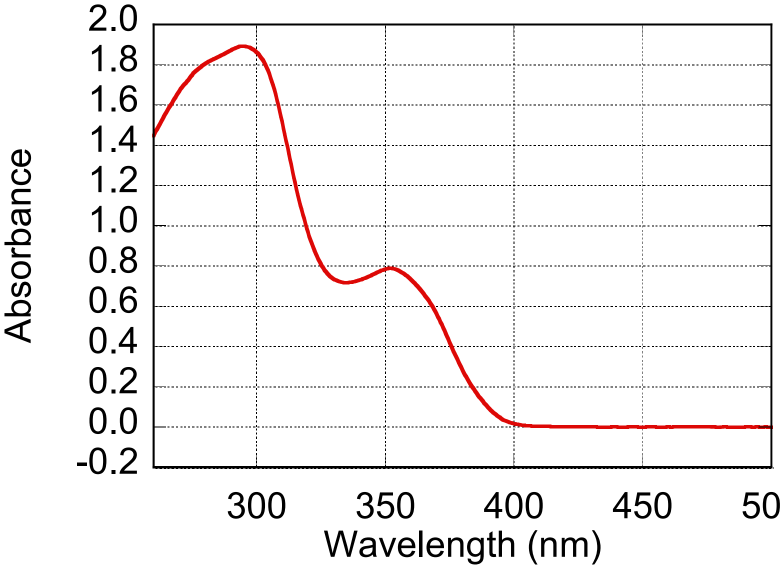

Figure S88. UV-vis absorption of **1** in 1,3-dichloropropane under 200 MPa (15.1×10^{-2} g/L, light path length = 2 mm).

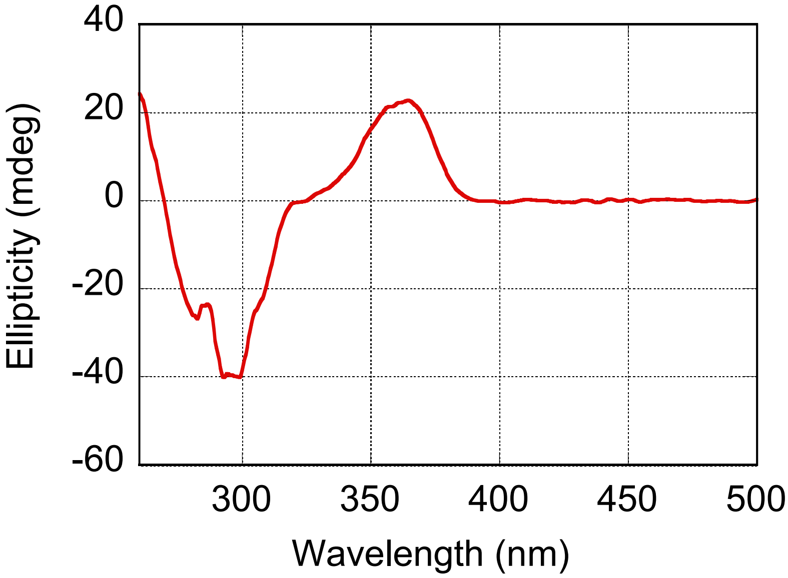

Figure S89. CD spectrum of **1** in 1,3-dichloropropane under 200 MPa (15.1×10^{-2} g/L, light path length = 2 mm).

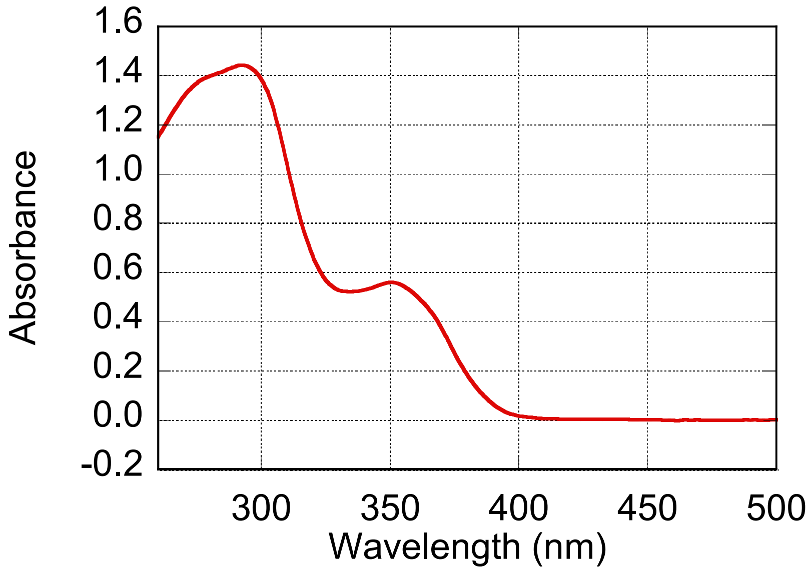

Figure S90. UV-vis absorption of **2** in 1,2-DCE under 0.1 MPa (15.1×10^{-2} g/L, light path length = 2 mm).

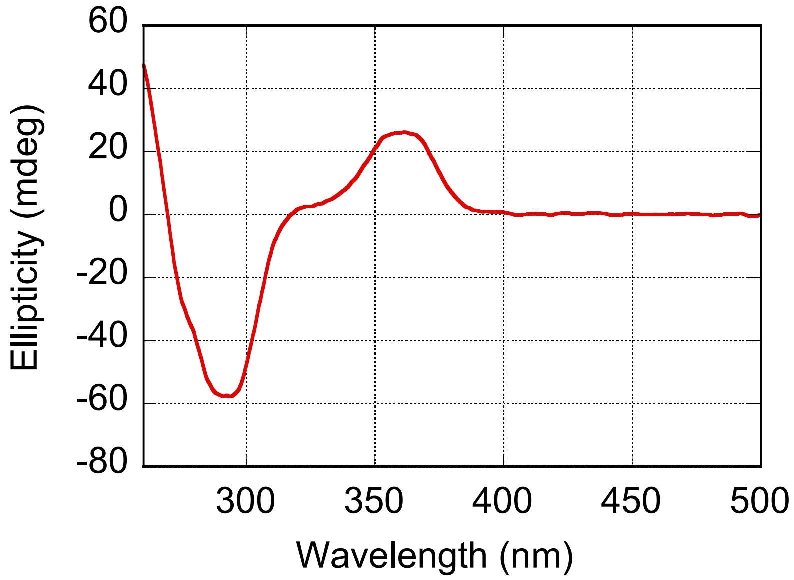

Figure S91. CD spectrum of **2** in 1,2-DCE under 0.1 MPa (15.1×10^{-2} g/L, light path length = 2 mm).

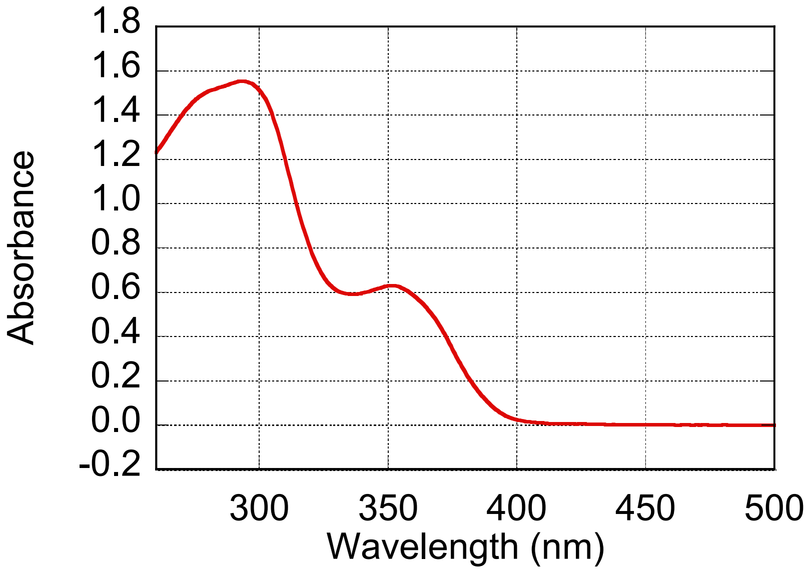

Figure S92. UV-vis absorption of **2** in 1,2-DCE under 200 MPa

(15.1 × 10^{-2} g/L, light path length = 2 mm).

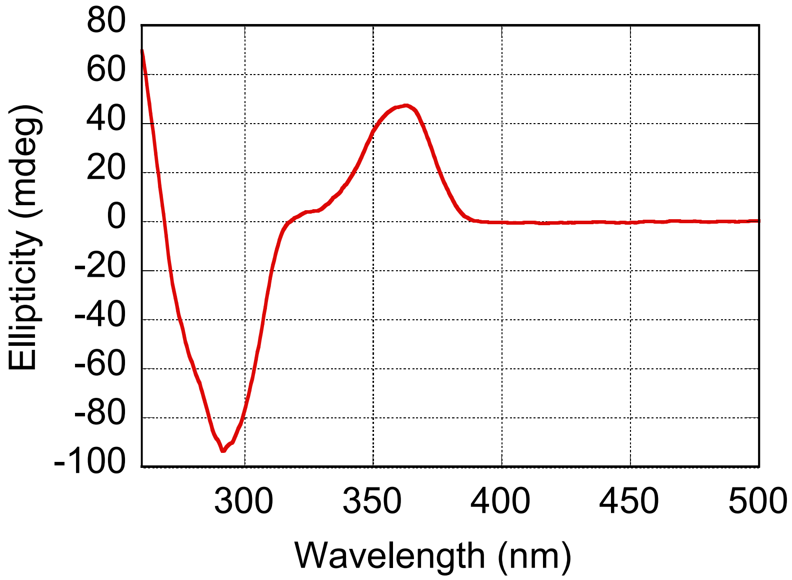

Figure S93. CD spectrum of **2** in 1,2-DCE under 200 MPa

(15.1 × 10^{-2} g/L, light path length = 2 mm).

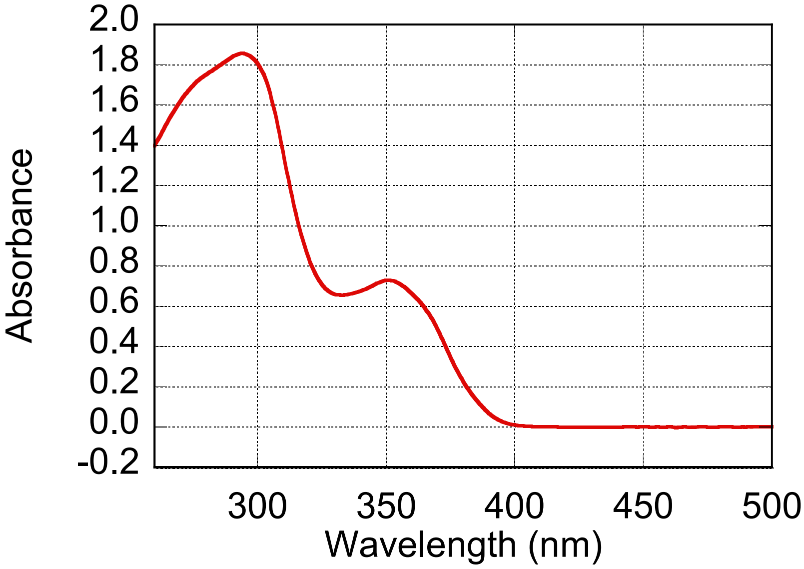

Figure S94. UV-vis absorption of **3** in 1,2-DCE under 0.1 MPa (16.7×10^{-2} g/L, light path length = 2 mm).

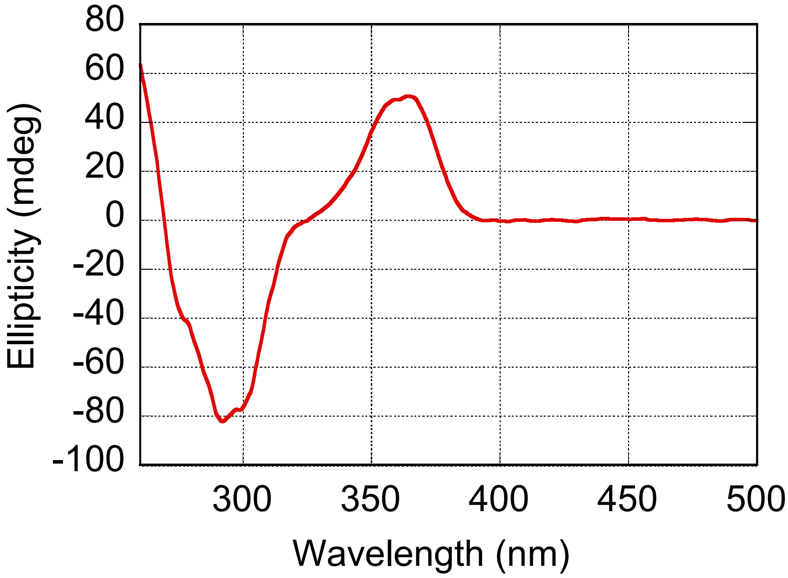

Figure S95. CD spectrum of **3** in 1,2-DCE under 0.1 MPa (16.7×10^{-2} g/L, light path length = 2 mm).

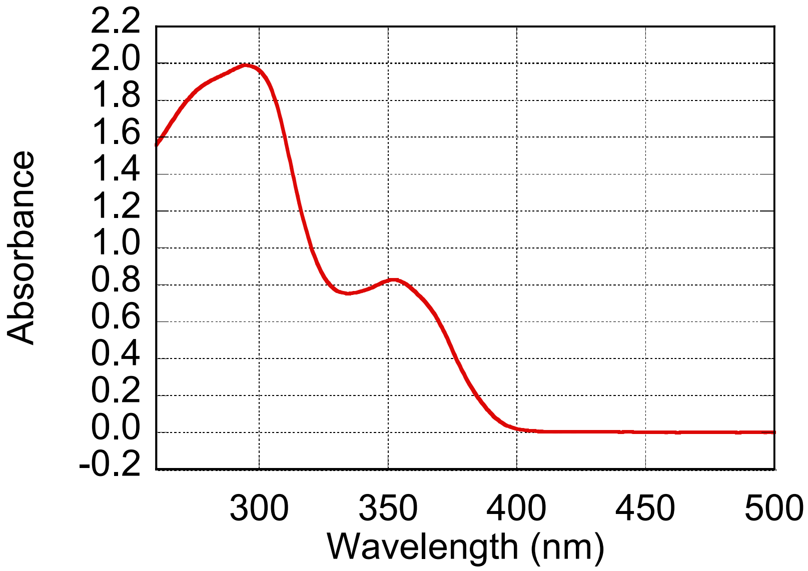

Figure S96. UV-vis absorption of **3** in 1,2-DCE under 200 MPa (16.7×10^{-2} g/L, light path length = 2 mm).

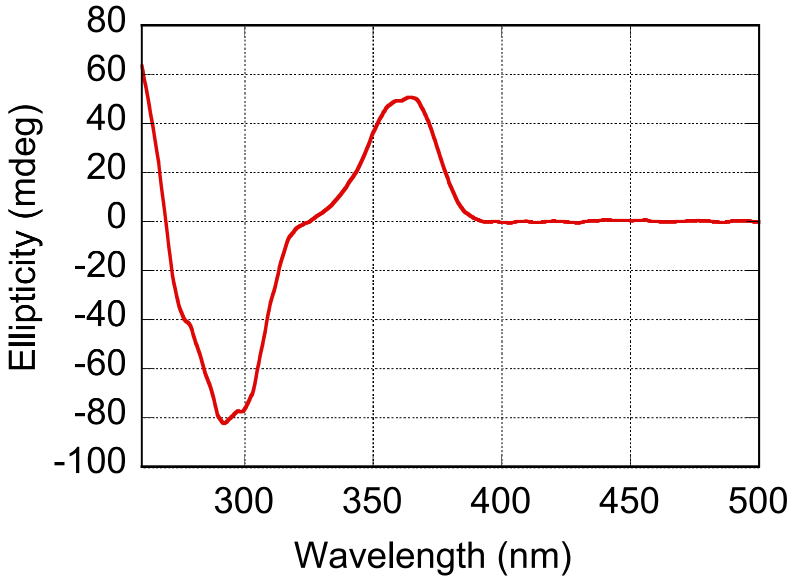

Figure S97. CD spectrum of **3** in 1,2-DCE under 200 MPa (16.7×10^{-2} g/L, light path length = 2 mm).

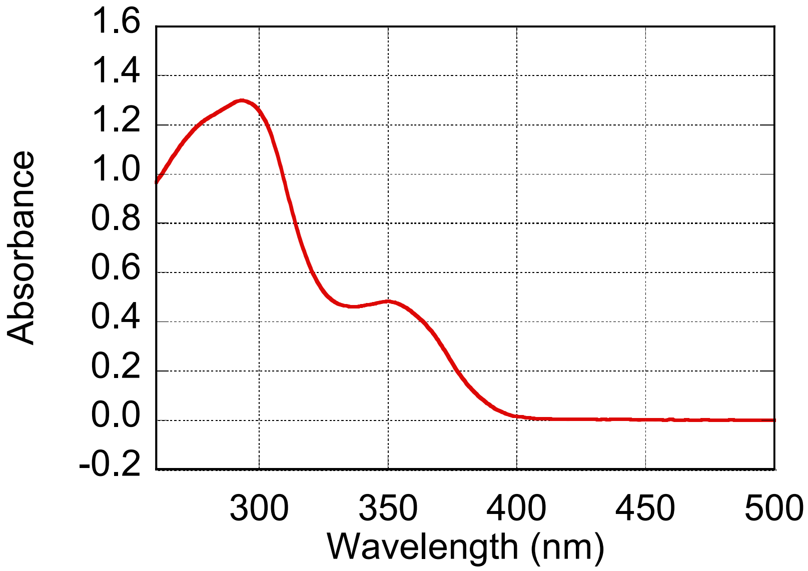

Figure S98. UV-vis absorption of **4** in 1,2-DCE under 0.1 MPa (13.2×10^{-2} g/L, light path length = 2 mm).

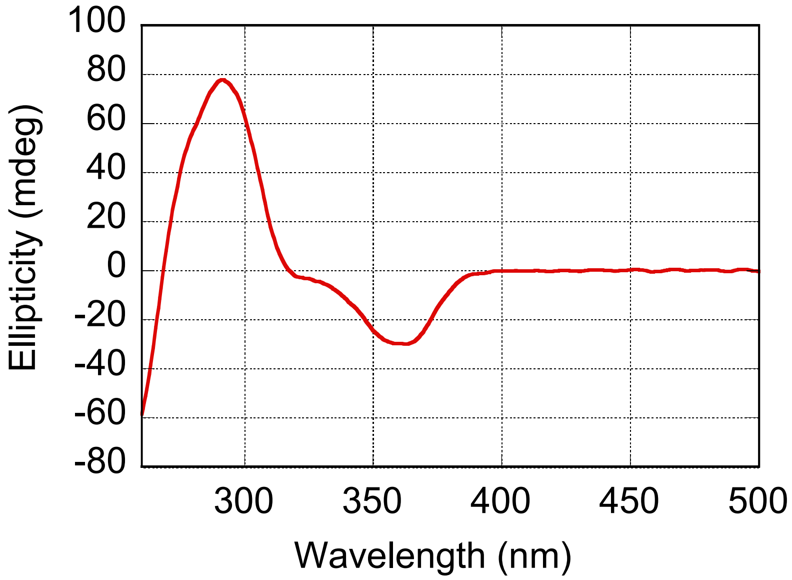

Figure S99. CD spectrum of **4** in 1,2-DCE under 0.1 MPa (13.2×10^{-2} g/L, light path length = 2 mm).

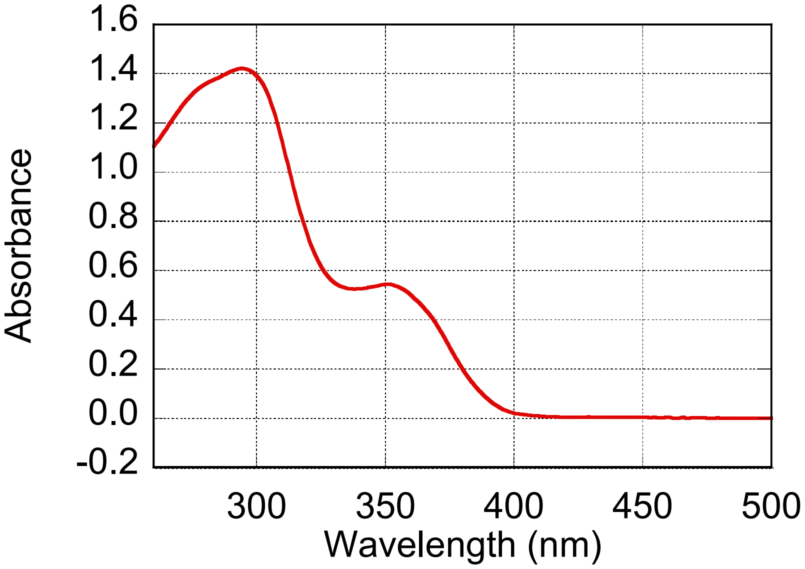

Figure S100. UV-vis absorption of **4** in 1,2-DCE under 200 MPa (13.2×10^{-2} g/L, light path length = 2 mm).

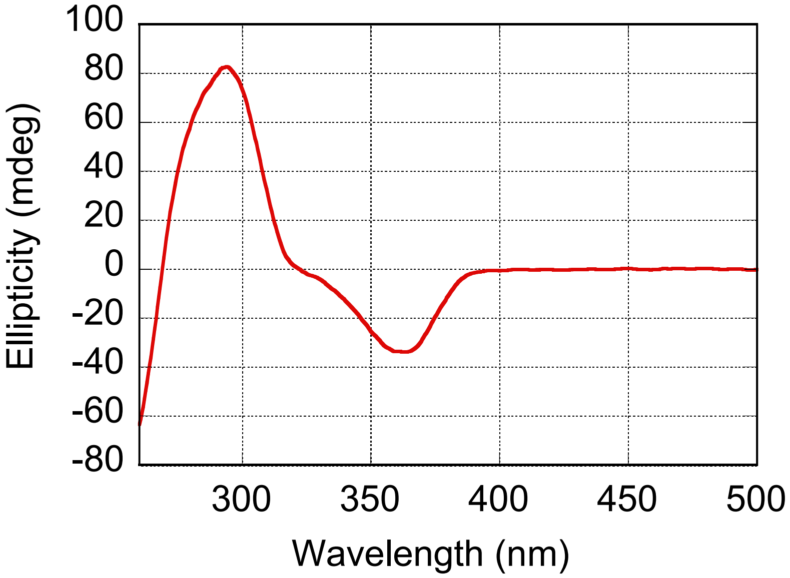

Figure S101. CD spectrum of **4** in 1,2-DCE under 200 MPa (13.2×10^{-2} g/L, light path length = 2 mm).